

Antidiabetic Activities of Triterpenoids Isolated from Bitter Melon Associated with Activation of the AMPK Pathway

Min-Jia Tan,^{1,5} Ji-Ming Ye,^{2,5} Nigel Turner,^{2,5} Cordula Hohnen-Behrens,² Chang-Qiang Ke,¹ Chun-Ping Tang,¹ Tong Chen,¹ Hans-Christoph Weiss,³ Ernst-Rudolf Gesing,⁴ Alex Rowland,² David E. James,^{2,*} and Yang Ye^{1,*}

¹State Key Laboratory of Drug Research, Shanghai Institute of Materia Medica, Shanghai Institutes for Biological Sciences, Chinese Academy of Sciences, Shanghai 201203, China

²Diabetes and Obesity Research Program, Garvan Institute of Medical Research, University of New South Wales, Sydney, NSW 2010, Australia

³Bayer Industry Services GmbH & Co., Leverkusen 51368, Germany

⁴Bayer CropScience AG, R & D, Agricultural Center, Monheim 40789, Germany

⁵These authors contributed equally to this work.

*Correspondence: d.james@garvan.org.au (D.E.J.), yye@mail.shcnc.ac.cn (Y.Y.)

DOI 10.1016/j.chembiol.2008.01.013

SUMMARY

Four cucurbitane glycosides, momordicosides Q, R, S, and T, and stereochemistry-established karaviloside XI, were isolated from the vegetable bitter melon (*Momordica charantia*). These compounds and their aglycones exhibited a number of biologic effects beneficial to diabetes and obesity. In both L6 myotubes and 3T3-L1 adipocytes, they stimulated GLUT4 translocation to the cell membrane—an essential step for inducible glucose entry into cells. This was associated with increased activity of AMP-activated protein kinase (AMPK), a key pathway mediating glucose uptake and fatty acid oxidation. Furthermore, momordicoside(s) enhanced fatty acid oxidation and glucose disposal during glucose tolerance tests in both insulin-sensitive and insulin-resistant mice. These findings indicate that cucurbitane triterpenoids, the characteristic constituents of *M. charantia*, may provide leads as a class of therapeutics for diabetes and obesity.

INTRODUCTION

Currently, there are 150 million people with diabetes worldwide, and this figure is expected to increase to over 300 million by 2025. This global pandemic is driven by type 2 diabetes (T2D) (Zimmet et al., 2001). Since insulin resistance is a major metabolic abnormality of T2D, there has been considerable interest in insulin-sensitizing agents to counteract insulin resistance for the treatment of this disease (Moller, 2001). Currently, pharmacological treatment of insulin resistance mainly targets two mechanisms: peroxisome-proliferator-activating receptors (PPARs) (Smyth and Heron, 2006) and AMP-activated protein kinase (AMPK) (Ye et al., 2005). The two most popular agents now in use are the thiazolidinediones (TZDs) and the biguanides. The TZDs are widely used but can have undesirable side effects (weight gain, fluid

retention, and heart failure). The biguanide metformin does not cause weight gain but mainly acts in liver rather than muscle and thus on its own is not a complete therapy. There is a worldwide search for better agents (Moller, 2001; Smyth and Heron, 2006).

Traditional medicines (TM) or complementary and alternative medicines are a fruitful source of future drugs to counteract insulin resistance, consistent with a resurgence of interest in drug discovery from natural products (Koehn and Carter, 2005). For example, metformin was a biguanide derivative of guanidine, originated from the plant Goat's Rue (*Galega officinalis*) as a structure-modified natural product to vastly improve its efficacy. A major advantage of TM is that they have been used to treat human diseases for many years and so there is considerable knowledge concerning in vivo efficacy and safety, two of the confounding problems facing other new chemical entities. However, in most cases there is little rigorous scientific evidence proving their efficacy and the mode of action is generally not known. To overcome these problems, it is essential to identify the active ingredients or molecules and investigate their specific effects in well-defined biological systems and animal models relevant to humans.

In this study, we have taken a targeted approach to investigate the active chemical molecules in *Momordica charantia* L. (Cucurbitaceae), also known as bitter melon, bitter gourd, or balsam pear. This plant is widely cultivated as a vegetable and medicinal herb in many Asian countries and has been shown to exert hypoglycemic effects in animal models and humans (Grover and Yadav, 2004). Although major chemical constituents of *M. charantia* include cucurbitane triterpenoids (Okabe et al., 1980, 1982a, 1982b; Miyahara et al., 1981; Murakami et al., 2001; Harinantenaina et al., 2006; Nakamura et al., 2006; Matsuda et al., 2007; Zhu et al., 1990), the precise active compounds responsible for the antidiabetic activity of this plant have not been clearly identified. In this work, we investigated the chemical constituents of *M. charantia* for the purpose of identifying the antidiabetic principles of this medicinal vegetable. Four novel cucurbitane glycosides, momordicosides Q, R, S, T, (**2**, **3**, **5**, **6**); the absolute-stereochemistry-established karaviloside XI (**1**); a spectroscopic-data-revised glycoside,

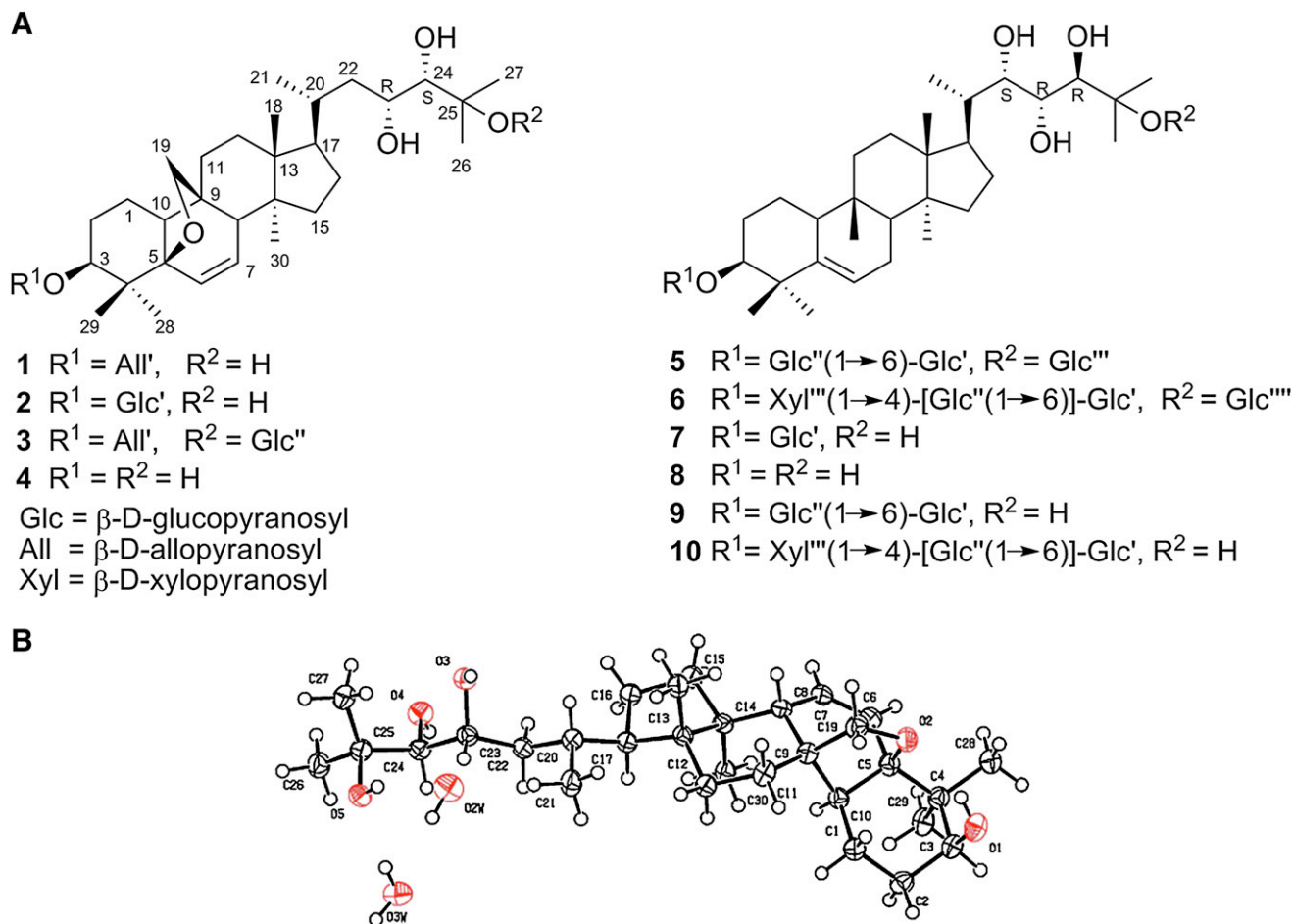


Figure 1. Chemical Structures of Cucurbitane Triterpenoids from Bitter Melon

(A) Chemical structures of cucurbitane triterpenoids from bitter melon.

(B) Perspective ORTEP drawing for compound **4**.

momorcharaside B (**7**); and two known triterpenoids, momordicoside A (**9**) and momordicoside B (**10**), were isolated (Figure 1A). These compounds, particularly **1** and **5**, and their aglycones (**4** and **8**), stimulated the translocation of the insulin-responsive glucose transporter GLUT4 to the plasma membrane in muscle and adipocyte cell lines. Intriguingly, these compounds also activated the AMP-activated protein kinase (AMPK) pathway, a major regulatory pathway for GLUT4 translocation (Huang and Czech, 2007). In vivo studies in mice showed a significant enhancement of glucose disposal and increases in fatty acid oxidation after acute administration of compound **5**. These results suggest that cucurbitane triterpenoids from *M. charantia* may provide novel leads for the development of a new class of AMPK-activating agents.

RESULTS

Structural Identification

Compound **1** was established as $\text{C}_{36}\text{H}_{60}\text{O}_{10}$ by HRESIMS (m/z 675.4064 $[M+\text{Na}]^+$). The plane structure of compound **1** was established as the recently reported karaviloside XI (Matsuda et al., 2007) on the basis of their identical NMR data. Mild acid hydrolysis of **1** furnished aglycone **4** and allose. The absolute configu-

ration of aglycone **4** was established by X-ray diffraction analysis (Figure 1B) and its biogenetic relationship. Thus, the structure of compound **1** was elucidated as 3-O- β -D-allopyranosyl-5 β ,19-epoxycucurbita-6-ene-23(*R*),24(*S*),25-triol.

Momordicoside Q (**2**) showed $[M+\text{Na}]^+$ at m/z 675.4113 ($\text{C}_{36}\text{H}_{60}\text{O}_{10}\text{Na}$) in the HRESIMS. Acid hydrolysis of compound **2** yielded aglycone **4** and glucose. ^1H NMR and ^{13}C NMR signals of compound **2** were superimposable on those of karaviloside XI (**1**) except for the variation of signals of the sugar moiety, which was inferred as β -D-glucose from its anomeric proton (δ_{H} 4.95, d, $J = 8.1$). According to these data, compound **2** was identified as 3-O- β -D-glucopyranosyl-5 β ,19-epoxycucurbita-6-ene-23(*R*),24(*S*),25-triol.

The molecular formula of momordicoside R (**3**) was $\text{C}_{42}\text{H}_{70}\text{O}_{15}$ revealed by HRESIMS (m/z 837.4632, $[M+\text{Na}]^+$), which was supported by ^{13}C NMR and distortionless enhancement by polarization transfer (DEPT) data. Allose and glucose were obtained by acid hydrolysis of compound **3**. ^{13}C NMR and DEPT spectra indicated the existence of six tertiary methyls, one secondary methyl, two olefinic carbons, six quaternary carbons, and ten methenes, three of which bore a hydroxyl group. The above ^{13}C NMR data as well as ^1H NMR data bore a resemblance to those of karaviloside

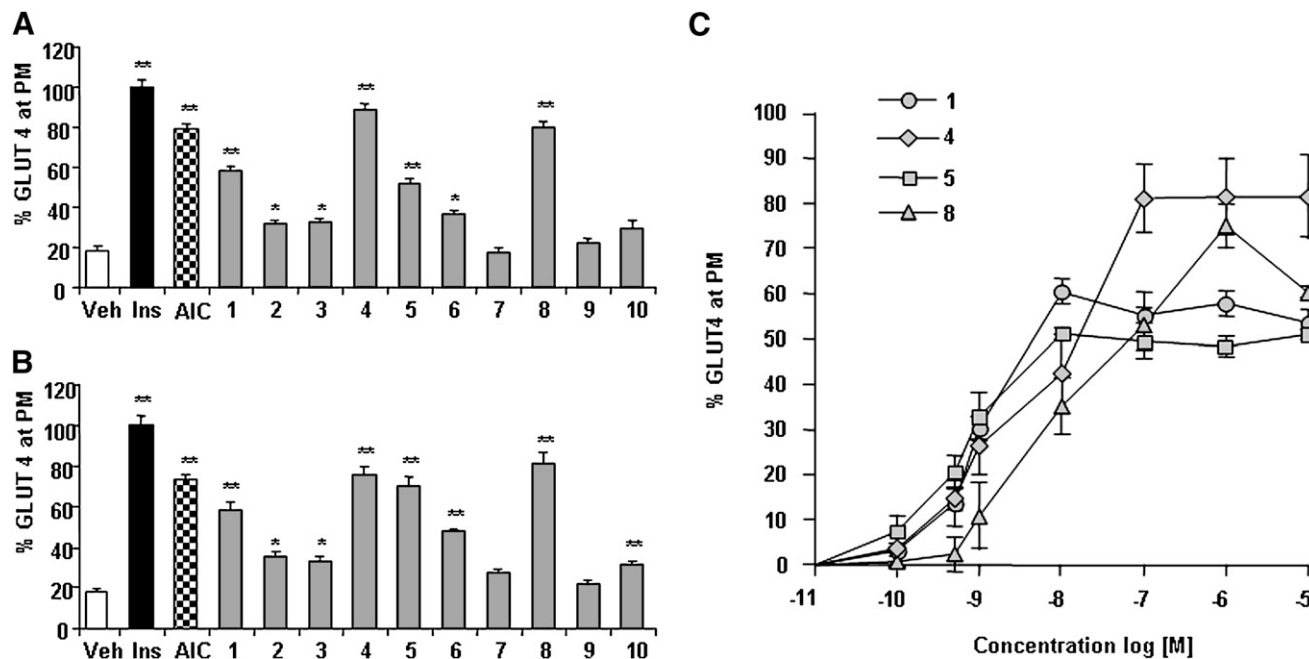


Figure 2. Effect of Cucurbitane Triterpenoids on GLUT4 Translocation in Cells

L6 myotubes (A) or 3T3-L1 adipocytes (B) were incubated with vehicle (Veh, DMSO containing saline, final concentration of DMSO: 0.2%), 100 nM insulin (In), 2 mM AICAR (AIC), or test compounds (10 μ M) for 30 min, and GLUT4 translocation from the cytosol to plasma membrane (PM) was measured as described in the Experimental Procedures. The dose-response curve was constructed in 3T3-L1 adipocytes for each compound at concentrations from 0.1 nM to 10 μ M (C) The results were quantified as a percentage of the maximum effect of insulin (100%) and expressed as means \pm SE. Three to four independent experiments were performed for each compound. * p < 0.05, ** p < 0.01 versus Veh control.

XI (1) with the exception of the appearance of six additional carbon signals for a monosaccharide moiety. Two anomeric proton signals, H-1' (δ_{H} 5.34, d, J = 7.7) and H-1'' (δ_{H} 5.21, d, J = 7.8), were assigned to β -D-allopyranosyl and β -D-glucopyranosyl moieties, respectively. ^1H -detected heteronuclear multiple-bond correlation (HMBC) experiment disclosed the long-range correlations between H-1' and C-3, and H-1'' and C-25, which established the linkage of each sugar moiety. The above evidence and analysis of heteronuclear single-quantum coherence (HSQC), HMBC, total correlated spectroscopy (TOCSY) spectra confirmed compound 3 as 3-O- β -D-allopyranosyl-25-O- β -D-glucopyranosyl-5 β ,19-epoxycucurbita-6-ene-23(R),24(S)-diol.

HRESIMS of momordicoside S (5) presented the molecular formula of $\text{C}_{48}\text{H}_{82}\text{O}_{20}$ (m/z 1001.5253 [$M+\text{Na}$] $^+$). ^1H NMR, ^{13}C NMR, and DEPT data showed the presence of seven tertiary methyls, one secondary methyl, a trisubstituted double bond, six quaternary carbons, seven aglycone methylenes, and three sugar methylenes, as well as three anomeric carbons, which suggested a triterpenoid glycoside with three sugar moieties. Enzymatic hydrolysis of compound 5 liberated aglycone 8 and glucose. Aglycone 8 was identical to the aglycone of momordicoside A (^1H NMR, ^{13}C NMR, DEPT, ESIMS, [α]), which was secured by the same hydrolysis procedure (Okabe et al., 1980). Thus, the absolute configuration of the aglycone 8 was established. The signals of three anomeric protons, H-1' (δ_{H} 4.75, d, J = 7.8), H-1'' (δ_{H} 5.12, d, J = 7.4), and H-1''' (δ_{H} 5.09, d, J = 7.3), indicated to three β -D-glucopyranosyl moieties. In addition, the HMBC correlations between C-3 and H-1', C-6' and H-1'', and C-25 and H-1''' were also observed. Based on the comprehensive

analysis of ^{13}C NMR, DEPT, HSQC, HMBC, and TOCSY spectra, the structure of momordicoside S (5) was formulated as 3-O- β -D-glucopyranosyl(1 \rightarrow 6)- β -D-glucopyranosyl]-25-O- β -D-glucopyranosyl-22(S),23(R),24(R),25-tetrahydroxycucurbit-5-ene.

HRESIMS afforded a possible molecular formula of momordicoside T (6) as $\text{C}_{53}\text{H}_{90}\text{O}_{24}$ (1113.5714, [$M+\text{Na}$] $^+$), which suggested a triterpenoid glycoside with four monosaccharide moieties. Xylose and glucose were released by acid hydrolysis of compound 6. Carbon signals from ^{13}C NMR and DEPT data were in good agreement with those of momordicoside S (5), except that five extra signals due to a xylopyranosyl moiety were observed. Four anomeric proton signals were assigned as β -D-glucopyranosyl moiety [H-1' (δ_{H} 4.71, d, J = 7.8)], β -D-glucopyranosyl moiety [H-1'' (δ_{H} 5.29, d, J = 6.6)], β -D-xylopyranosyl moiety [H-1''' (δ_{H} 5.30, d, J = 7.2)], and β -D-glucopyranosyl moiety [H-1'''' (δ_{H} 5.10, d, J = 7.8)] from its ^1H NMR spectrum, respectively. The oligoglycoside structure of compound 6 was characterized by HMBC correlation: H-1' and C-3, H-1'' and C-6', H-1''' and C-4', H-1'''' and C-25. Based on the above spectroscopic evidence, together with TOCSY spectrum, structure of compound 6 was determined to be 3-O- β -D-xylopyranosyl(1 \rightarrow 4)- β -D-glucopyranosyl(1 \rightarrow 6)]- β -D-glucopyranosyl]-25-O- β -D-glucopyranosyl-22(S),23(R),24(R),25-tetrahydroxycucurbit-5-ene.

The spectroscopic data of momorcharaside B (7) reported by Zhu et al. were not consistent with the described structure (Zhu et al., 1990). Herein, we revised the spectroscopic data of momorcharaside B. Its molecular formula $\text{C}_{36}\text{H}_{62}\text{O}_{10}$ was derived from HRESIMS (m/z 677.4224, [$M+\text{Na}$] $^+$). Acid hydrolysis of momorcharaside B with 2% aqueous HCl-dioxane (1:1, v/v)

gave glucose and aglycone **8**. Six glucopyranosyl carbon signals disappeared by contrast with those of momordicoside A. β -D-configuration of the sugar moiety was discerned from the coupling constant of anomeric proton ($J = 7.7$). Consequently, its structure was formulated as 3-O- β -D-glucopyranosyl-22(S),23(R),24(R),25-tetrahydroxycucurbit-5-ene by ^1H NMR, ^{13}C NMR and DEPT spectra.

Assessment of Antidiabetes Properties in Cells

In order to assess the potential activity of these compounds on glucose metabolism and insulin action, we first examined their effects on the translocation of the glucose transport GLUT4 to the plasma membrane, because this is an essential step for inducible glucose uptake into muscle and fat cells. The results showed that most compounds exhibited the same pattern of biologic activity to stimulate GLUT4 translocation in L6 muscle cells (Figure 2A) and 3T3L1 adipocytes (Figure 2B), and among them **1**, **4**, **5**, and **8** increased GLUT4 translocation by 3- to 4-fold, an efficacy close to the maximum effect of insulin (5-fold) and AICAR (~4-fold). The dose-response curves (Figure 2C) showed that compounds **1**, **4**, **5**, and **8** exhibited this biological activity at concentrations as low as 0.1 nM and reached their maximal effects at between 10 and 100 nM.

GLUT4 translocation is mainly regulated by two independent pathways: the insulin signaling pathway and the AMP-activated protein kinase (AMPK) pathway (Huang and Czech, 2007). The phosphatidylinositol 3' kinase (PI3K)/Akt pathway is known to play a major regulatory role in the insulin action pathway, and PI3K inhibitors such as wortmannin, inhibit insulin stimulated GLUT4 translocation. The stimulatory effects of cucurbitane triterpenoids on GLUT4 translocation were not affected by wortmannin (Figure 3A). Moreover, in contrast to that observed with insulin, these compounds had no significant effect on phosphorylation of Akt phosphorylation, a downstream substrate of PI3K (Figure 3B). These data indicate that the stimulatory effects of cucurbitane triterpenoids on GLUT4 translocation are not likely to be mediated via the PI3K/Akt pathway.

The stress kinase, AMPK, has also been shown to regulate GLUT4 translocation (Huang and Czech, 2007), and hence we investigated whether the cucurbitane triterpenoids activate AMPK. In 3T3-L1 adipocytes we observed increased phosphorylation (Thr172) of AMPK with compounds **1**, **4**, **5**, and **8** (Figure 4A) to a level comparable with the well-described AMPK agonist AICAR (Figure 4B). Consistent with our data for GLUT4 translocation, AMPK phosphorylation was not induced by these compounds at a concentration of 0.1 nM, but was elevated at 100 nM to 10 μM (Figure 4B). We also observed increased AMPK phosphorylation in L6 myotubes by compounds **1**, **4**, **5**, and **8**, again to a relatively similar level to AICAR (Figures 4C and 4D).

Assessment of Antidiabetes Properties in Animals

On the basis of these in vitro data, we examined whether this class of compounds had any beneficial effects on glucose and fuel metabolism in vivo. For these studies, we restricted our analysis to compounds **5** and/or **6** because we were not able to isolate the other compounds in sufficient quantity for in vivo administration. We first examined whole-body energy expenditure and fat oxidation in the resting state. The results (Figure 5) showed a small increase in energy expenditure (indicated by increased

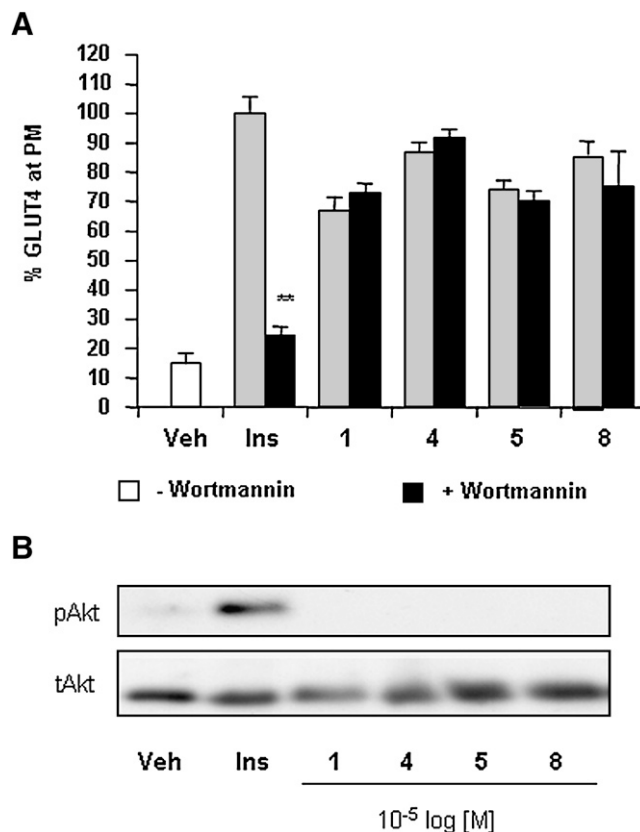


Figure 3. Effects of Compounds 1, 4, 5, and 8 on Insulin Signaling Pathways

Experiments were performed in 3T3-L1 adipocytes and values represent means \pm SE. Cells were incubated with 100 nM insulin, 10 μM test compounds in the presence of vehicle (Veh, DMSO containing saline, final concentration of DMSO: 0.2%) or 10 μM wortmannin.

(A) GLUT4 transduction during inhibition of insulin signal transduction from three to four independent experiments ($*p < 0.05$, $**p < 0.01$ versus Veh).

(B) Immunoblots for phospho-Akt (Ser473) and Akt in 3T3-L1 adipocytes (representative blots of three repeats). Cells were incubated with Veh, 100 nM insulin or test compounds (at 10 μM each) for 30 min.

oxygen consumption, VO_2) at around 30 min and 7.5 hr after the administration of compound **5** (100 mg/kg) as compared to vehicle (0.9% saline). Strikingly, there was a substantial increase in fat oxidation (indicated by decreased respiratory exchange ratio, RER) with compound **5** during this entire period of time. These effects are comparable to those induced by AICAR at 250 mg/kg.

We further examined the effects of compounds **5** and **6** on whole-body glucose metabolism. Compound **5** had no significant effect on basal blood glucose levels (Figure 6A). However, we did observe a significant increase in glucose clearance during an intraperitoneal glucose tolerance test. Under the same conditions, AICAR at a dose of 500 mg/kg (but not at 250 mg/kg; data not shown) had a modest effect on glucose tolerance. Thus, these data indicate that the cucurbitane triterpenoids are significantly more potent in vivo than a traditional AMPK agonist. Although metformin had a small effect to reduce blood glucose (from 6.30 ± 0.17 to 5.27 ± 0.21 mM, $p < 0.05$, $n = 8$) at the tolerable dose (200 mg/kg), it did not have any significant effect on glucose disappearance during the ipGTT. In order to examine

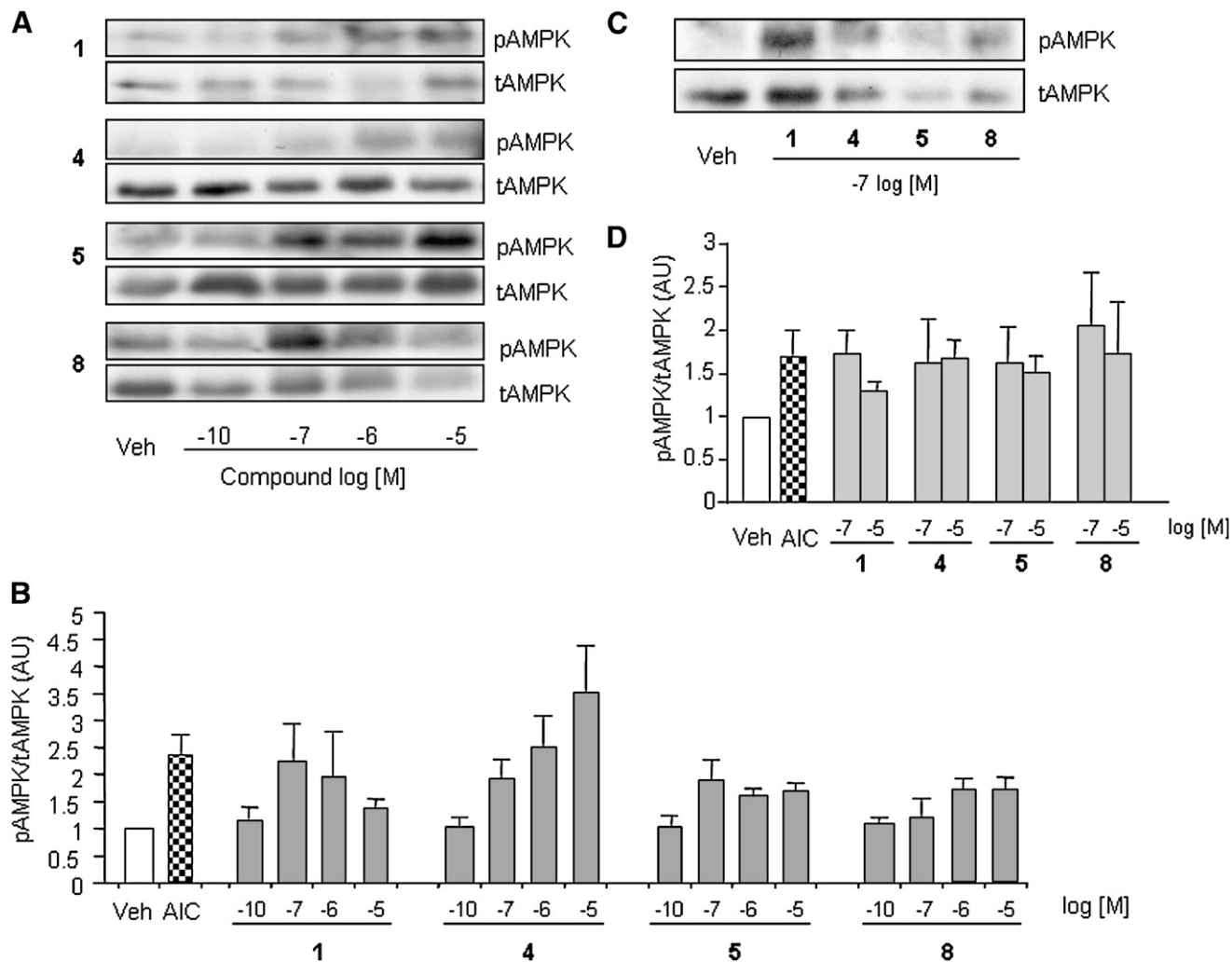


Figure 4. Effects of Compounds 1, 4, 5, and 8 on AMPK Phosphorylation

3T3-L1 and L6 cells were treated with test compounds as described in the [Experimental Procedures](#) and equal amounts of lysates were resolved by SDS-PAGE and immunoblotted for AMPK and phospho-AMPK (Thr172).

(A) Representative blots for compounds 1, 4, 5 and 8 in 3T3-L1 adipocytes.

(B) Quantification of the ratio of phospho-AMPK to total AMPK from three independent experiments (means \pm SE).

(C) Representative blots for compounds 1, 4, 5 and 8 in L6 myotubes at 0.1 μ M.

(D) Quantification of the ratio of phospho-AMPK to total AMPK from three independent experiments in L6 myotubes (means \pm SE).

whether cucurbitane triterpenoids also acutely improve glucose tolerance in the insulin-resistant state, we tested the effect of compound 6 (10 mg/kg) in high-fat-fed mice. As shown in [Figure 6B](#), compound 6 resulted in a significant improvement in glucose tolerance in high-fat-fed animals.

DISCUSSION

Bitter melon is one of the most popular dietary botanicals for the treatment of diabetes mellitus, though the responsible active components are not clearly elucidated. It has been widely reported that its antidiabetic metabolites are the mixture of polypeptides, glycosides, alkaloids, and sterols. Earlier studies appear to indicate that polypeptide-p of *M. charantia* has hypoglycemic effects in gerbils, langurs, and human ([Khanna et al., 1981](#)). Recent studies have suggested the antidiabetic proper-

ties of bitter melon extracts in insulin-target tissues such as skeletal muscle and adipose tissues ([Grover and Yadav, 2004](#)). However, the antidiabetic activity of cucurbitane triterpenoids, the characteristic chemical constituents of *M. charantia*, is not well defined. Only two cucurbitane triterpenes were reported to show blood hypoglycemic effects in the alloxan-injected mice at 400 mg/kg ([Harinantenaina et al., 2006](#)). However, it should be noted that the diabetic animal model used in this study was very mild. Moreover, the biologic mechanisms involved in their antidiabetic properties are not clear. Particularly, our study focused on the structure identification, and biological evaluation of four novel cucurbitane glycosides, momordicosides Q, R, S, T (2, 3, 5, 6), karaviloside XI (1), and their aglycones.

We have revealed two classes of cucurbitane triterpenoids (1–10), both of which stimulate GLUT4 translocation in adipocytes and muscle cells and both of which stimulate the activity

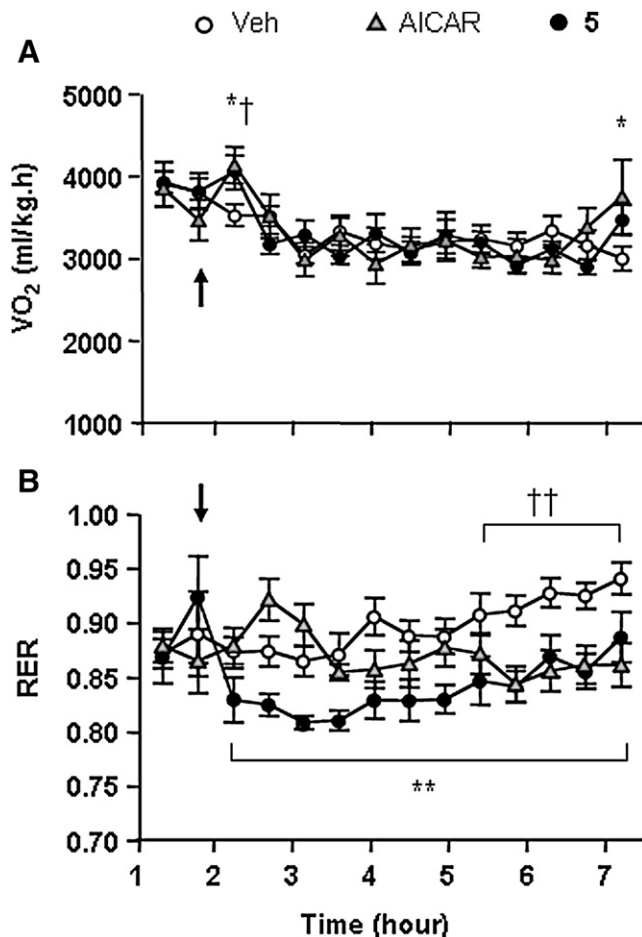


Figure 5. Effects of Compound 5 on Whole-Body VO_2 and RER in Mice

(A and B) Mice were placed in a metabolic chamber at 9:00 a.m. and after 2 hr of rest compound 5 (100 mg/kg), AICAR (250 mg/kg), or saline (Veh) was injected subcutaneously into the mice. * $p < 0.05$, ** $p < 0.01$ versus Veh; † $p < 0.05$, †† $p < 0.01$ 5 versus Veh ($n = 6$ –8/group).

of the AMPK pathway. Among these compounds, we have identified two glycosides, karaviloside XI (**1**) and momordicoside S (**5**), that show the most significant potency. Interestingly, aglycones of these two compounds also show similar biologic properties, which suggest that cucurbitane aglycones may be the important pharmacophore for the antidiabetic activity.

To screen the antidiabetic properties of these compounds, we chose GLUT4 translocation in muscle cells and adipocytes as the primary system. This screen measures the movement of the insulin responsive glucose transporter GLUT4 to the cell surface, an essential step for insulin-responsive glucose transport in muscle and adipose tissue that becomes defective in insulin resistance (Huang and Czech, 2007). We found that most of the tested compounds in the cucurbitane triterpenoid class, particularly **1**, **4**, **5**, and **8**, exhibited a strong effect to stimulate GLUT4 translocation by several fold in both cell types to a level that was comparable to maximal insulin and AICAR stimulation. Of particular note, the concentration required for compounds **1**, **4**, **5**, and **8** to reach their maximal effect was approximately

10,000 times lower compared to AICAR (0.1 μ M for **1**, **4**, **5**, and **8** versus 1–2 mM for AICAR). These results indicate that cucurbitane triterpenoids are highly potent and efficacious in stimulating GLUT4 translocation in insulin responsive cells.

To investigate the mechanism responsible for the stimulated GLUT4 translocation by these compounds, we examined their effects on the cellular signaling pathways that are known to mediate this process. Our findings clearly demonstrate that in contrast to previous studies (Grover and Yadav, 2004), these compounds do not activate the PI3K/Akt pathway in cells and their ability to stimulate GLUT4 translocation was insensitive to the PI3K inhibitor wortmannin. We further investigated whether the AMPK pathway is involved because this pathway is another major regulator of GLUT4 translocation during exercise or in response to some antidiabetic agents such as AICAR and metformin (Huang and Czech, 2007). Indeed, these triterpenoids were able to increase the phosphorylation of AMPK to a relatively similar level to AICAR, suggesting that the AMPK signaling pathway is likely responsible for the stimulation of GLUT4 translocation by this class of compounds.

The identification of the AMPK pathway as a likely mechanism for the stimulation of GLUT4 translocation by triterpenoids from *M. charantia* is particularly interesting in relation to diabetes and obesity because activation of AMPK increases fatty acid oxidation, inhibits lipid synthesis, and can improve insulin action (Ye et al., 2005; Iglesias et al., 2002). Based on a number of studies showing that AMPK regulates a variety of different metabolic pathways, it is widely recognized as a useful and safe target for the treatment of metabolic disorders such as T2D and dyslipidemia (Ye et al., 2005; Musi, 2006). Hence, our findings of the activation of the AMPK pathway by these compounds may implicate these triterpenoids as a novel class of molecules with therapeutic potential for insulin resistant states by targeting AMPK.

One of the difficulties in pursuing the mechanism of action of these isolated compounds at the present stage is their limited availability due to the complicated secondary metabolites from *M. charantia*. Despite this, we were able to scale up isolation of S (**5**) and T (**6**) to produce amounts sufficient for limited acute studies in animals. Consistent with the *in vitro* studies implicating the AMPK pathway, we observed that momordicoside S (**5**) was able to stimulate whole-body fat oxidation in mice, with a minor increase in energy expenditure. The AMPK activator AICAR has been shown to acutely lower plasma glucose and ameliorate insulin resistance in high-fat-fed rats (Iglesias et al., 2002). Based on our findings described above, we predicted that cucurbitane triterpenoids may have similar effects on glucose metabolism *in vivo*. Indeed, we found that both momordicoside S (**5**) and T (**6**) significantly enhanced glucose tolerance in normal mice, and the efficacy was comparable to that produced by AICAR at a 5- to 50-fold higher dose. Interestingly, neither a tolerable intraperitoneal dose of metformin nor a reduced dose of AICAR (250 mg/kg; data not shown) had any detectable effect on glucose tolerance. These findings are consistent with the results on GLUT4 translocation and AMPK activity *in vitro* and show that cucurbitane triterpenoids identified in the present study have increased potency to improve glucose tolerance in mice compared with commonly used AMPK activators AICAR or metformin. Compound **6** was also able to acutely improve glucose

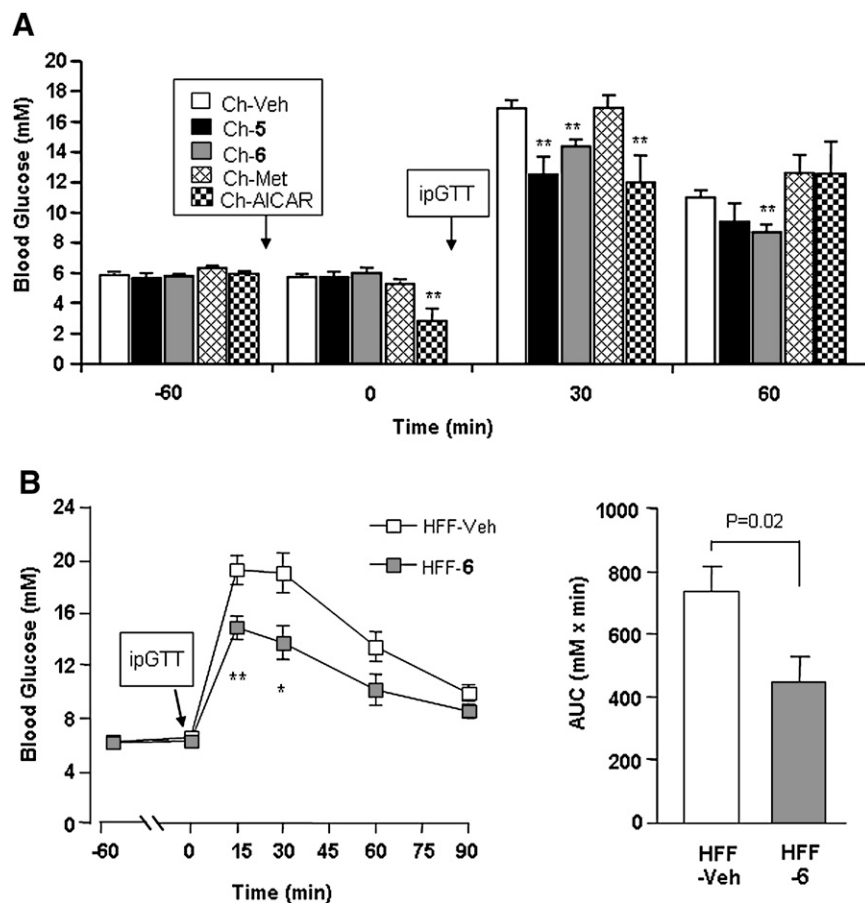


Figure 6. Acute Effects of Compounds 5 and 6 on Blood Glucose in Mice

(A) Standard chow-fed (Ch) mice fasted for 5–7 hr were used for the experiments. Following a basal blood sample at –60 min, vehicle (100 μ l of 15% glycerol, 5% ethanol and 80% saline), compound 5 (100 mg/kg), compound 6 (at a lower dose: 10 mg/kg), AICAR (500 mg/kg), or metformin (200 mg/kg) was injected intraperitoneally (ip). A second sample of blood was taken around 0 min to assess followed an immediate ip glucose tolerance test (ipGTT) at a glucose load of 3.0 g/kg in insulin sensitive Ch-fed mice.

(B) The effect on blood glucose in insulin-resistant, high-fat-fed (HFF) mice. The ipGTT was performed at a glucose load of 2.0 g/kg. * $p < 0.05$, ** $p < 0.01$ versus corresponding vehicle controls ($n = 7$ –9/group).

tolerance in high-fat-fed mice, suggesting therapeutic potential of these cucurbitane triterpenoids for the treatment of insulin resistance. Based on their *in vitro* effects, we suspect that other compounds of this class may have similar effects.

It is intriguing that many compounds that appear to have beneficial effects in the treatment of insulin resistance do so at least in part via activating AMPK activity. In particular, metformin (Zhou et al., 2001) and berberine (Lee et al., 2006), two plant-derived compounds that have been described to increase insulin sensitivity and reduce body weight, both activate AMPK. Interestingly, both metformin and berberine have also been described as weak mitochondrial poisons, and so it is believed that elevated intracellular AMP levels ensuing as a function of reduced mitochondrial respiration may trigger increased AMPK activity (Brunmair et al., 2004; Pereira et al., 2007). In this context, it is interesting that the upstream AMPK kinase, LKB1, is required for AMPK activation by metformin and its subsequent therapeutic effects *in vivo* (Shaw et al., 2005). We have observed no activation of AMPK by compounds 1, 4, 5, and 8 in HeLa cells (data not shown) which lack LKB1, suggesting that these triterpenoid compounds may activate AMPK in a similar fashion to metformin. However, it is important to mention that we have not observed any toxic effects of these compounds in either cells in culture or in animals, suggesting that if they do affect mitochondrial integrity, these effects are likely to be quite mild.

In view of the potency of the cucurbitane triterpenoids on glucose metabolism, it will be of great interest to determine the pri-

mary targets of these compounds leading to the activation of AMPK. One possibility might be that they act at intracellular target(s) after entering cells by some active transport system as the structural features of glycosides may render them as substrates for naturally occurring transporters (Lipinski et al., 2001). For example, cardiac sodium pumps are the receptors for classical cardiac glycosides such as digitalis, and there is a report which shows that ginsenoside Rg1 can be transported into epithelial cells with

peak concentration of 1.28 mg/ 10^5 cells at 0.5 hr (Meng et al., 2007). Alternatively, cucurbitane triterpenoids may bind to cell-surface receptors, initiating an intracellular signaling pathway analogous to that seen with other biological molecules such as leptin and adiponectin. Future studies will be required to distinguish between these possibilities.

SIGNIFICANCE

The structures and absolute configurations of four novel cucurbitane glycosides, momordicosides Q, R, S, and T, and karaviloside XI (1) were elucidated on the basis of spectroscopic data, chemical degradation, and X-ray diffraction analyses. Momordicoside S (5), karaviloside XI (1), and their aglycones (4 and 8), exhibited a number of biologic effects in cells. In both L6 myotubes and 3T3-L1 adipocytes, they stimulated GLUT4 translocation from cytosol to the cell membrane. This effect was associated with an increase in the activity of AMP-activated protein kinase. Consistent with these *in vitro* effects, administration of momordicoside S (5) into mice significantly enhanced glucose disposal from the circulation and promoted fatty acid oxidation. Additionally, we have demonstrated significant amelioration of glucose intolerance by momordicoside T (6). Based on our review of the literature, there are approximately 70 reported cucurbitane triterpenoids, and our UPLC/ESIMS analyses of the extracts of bitter melon suggest their high abundance in

Table 1. ^{13}C and ^1H NMR Data of Compounds 2, 3, 5–7 in $\text{C}_5\text{D}_5\text{N}$

	δ_{C}					δ_{H}				
	2 ^a	3 ^b	5 ^b	6 ^b	7 ^a	2 ^c	3 ^d	5 ^d	6 ^d	7 ^c
1	18.9	18.5	22.6	22.5	22.6	1.30 1.78	1.31 1.72	1.52 1.78	1.46 1.78	1.58 1.76
2	27.6	27.2	29.1	29.0	29.1	1.76 2.36	1.74 2.32	1.90 2.50	1.20 2.38	1.92 2.50
3	85.4	85.2	87.3	87.3	87.7	3.70 br s	3.64 br s	3.53 br s	3.66 br s	3.86 br s
4	39.1	38.6	41.6	41.6	41.8					
5	85.8	85.8	143.2	143.1	143.2					
6	134.2	133.8	118.6	118.7	118.7	6.21 (10.5)	6.14 dd (1.3 8.3)	5.37 d (4.4)	5.42 d (4.2)	5.4 d (4.8)
7	130.0	130.1	24.5	24.5	24.6	5.54 dd (3.7 9.0)	5.5 dd (3.3 9.8)	1.62 2.18	1.70 2.24	1.64 2.27
8	52.3	51.9	43.7	43.7	43.8	2.25	2.26	1.58	1.66	1.60
9	45.3	44.9	34.6	34.6	34.7					
10	40.1	39.7	38.4	38.3	38.5	2.25	2.24	2.16	2.22	2.18
11	23.9	23.5	32.4	32.4	32.5	1.30 1.58	1.29 1.58	1.28 1.52	1.34 1.56	1.32 1.54
12	31.2	30.7	30.7	30.6	30.8	1.52 1.56	1.44 1.54	1.46 1.54	1.52 1.60	1.48 1.58
13	45.6	45.2	46.7	47.3	46.8					
14	48.9	48.6	49.0	49.1	49.2					
15	33.3	32.9	35.2	35.2	35.3	1.10 1.15	1.09 1.14	1.04 1.14	1.12 1.22	1.15 1.23
16	28.5	28.1	27.6	27.7	27.8	1.38 1.92	1.36 1.86	1.48 2.34	1.56 2.42	1.58 2.48
17	51.6	51.2	47.8	47.7	47.7	1.48	1.44	1.95	2.00	2.02
18	15.0	14.6	15.4	15.3	15.3	0.77 s	0.74 s	0.82 s	0.83 s	0.89 s
19	80.1	79.8	28.1	28.0	28.2	3.57 d (8.3) 3.7 d (8.3)	3.56 d (7.7) 3.74 d (7.7)	0.80 s	0.81 s	0.85 s
20	32.7	32.3	42.8	42.8	43.1	2.09	2.04	2.14	2.20	2.22
21	18.9	18.5	14.9	14.9	14.8	1.12 d (6.1)	1.06 d (6.0)	1.38 d (6.6)	1.37 d (6.6)	1.44 d (6.6)
22	43.3	42.3	71.3	71.3	72.5	1.22 2.38	1.14 2.26	4.59 d (3.6)	4.66	4.60
23	67.7	66.6	71.4	71.3	71.2	4.59	4.48	4.18	4.24	4.14
24	79.9	79.7	74.1	74.1	75.4	3.56	3.61	4.28	4.36	4.46
25	73.6	81.0	81.5	81.5	74.4	1.65 s	1.72 s	1.81 s	1.82 s	1.70 s
26	28.0	23.0	23.2	23.3	24.2	1.67 s	1.73 s	1.70 s	1.71 s	1.68 s
27	27.0	24.6	24.0	24.1	29.1	1.56 s	1.45 s	1.43 s	1.44 s	1.53 s
28	21.1	20.5	25.8	25.7	26.0	0.87 s	0.86 s	1.00 s	1.03 s	1.09 s
29	25.6	25.2	28.4	28.4	28.5	0.93 s	0.83 s	0.78 s	0.78 s	0.83 s
30	20.2	19.8	18.1	18.0	18.1	1.12 d (6.1)	1.06 d (6.0)	1.38 d (6.6)	1.37 d (6.6)	1.44 d (6.6)
1'	106.7	104.0	106.9	106.8	107.4	4.95 (8.1)	5.34 d (7.7)	4.75 d (7.8)	4.71 d (7.8)	4.9 d (7.7)
2'	75.8	72.7	75.2	76.2	75.5	4.02	3.92	3.84	4.12	3.98
3'	78.3	72.3	78.4	74.8	78.7	4.03	4.67	3.89	3.81	4.00
4'	71.9	68.9	71.5	80.0	71.8	4.25	4.14	4.05	4.28	4.22
5'	78.4	75.8	77.3	75.0	78.2	4.02 6	4.44	4.02	4.00	4.24
6'	63.1	62.9	70.1	68.4	63.1	4.45 4.58	4.32 4.50	4.24 4.76	4.62 4.84	4.4 4.59
1''		98.5	105.1	105.1			5.21 d (7.8)	5.12 d (7.4)	5.29 d (6.6)	
2''		75.0	75.2	75.0			3.96	3.98	4.00	
3''		78.5	78.4	78.4			4.22	3.90	3.96	
4''		71.5	71.5	71.4			4.16	4.18	4.14	
5''		78.0	78.3	78.4			3.93	4.18	4.18	
6''		62.5	62.6	62.6			4.32 4.52	4.30 4.47	4.34 4.54	
1'''			97.6	105.1				5.09 d (7.3)	5.30 d (7.2)	
2'''			75.1	75.0				4.00	3.94	
3'''			78.4	78.4				3.79	4.24	
4'''			71.4	70.8				3.91	4.16	
5'''			78.7	67.1				4.10	3.85 4.17	
6'''			62.6					4.20 4.40		
1''''				97.6					5.10 d (7.8)	

Table 1. Continued

	δ_C					δ_H	2^c	3^d	5^d	6^d	7^c
	2^a	3^b	5^b	6^b	7^a						
$2'''$				75.2						4.00	
$3'''$				78.4						3.84	
$4'''$				71.4						4.14	
$5'''$				78.7						4.16	
$6'''$				62.6						4.28 4.46	

ppm, J in Hz.^a 100 MHz.^b 150 MHz.^c 400 MHz.^d 600 MHz.

this plant. Along with this, their extremely high potency indicates that cucurbitane triterpenoids are likely to be major contributors to the antidiabetic effects of bitter melon. Importantly, we have identified AMPK as a potential mediator of the cucurbitane triterpenoids for their stimulation of GLUT4 translocation in muscle and fat cells. The present study provides an important basis for further analysis of structure-activity relationship to develop optimized leads from cucurbitane triterpenoids for the treatment of insulin resistance and obesity.

EXPERIMENTAL PROCEDURES

General Experimental Procedures

Optical rotations were taken on a Perkin-Elmer 341 polarimeter. IR spectra were recorded on Nicolet Magna FT-IR 750 spectrophotometer using KBr disks. NMR spectra were recorded on Bruker AM-400 and INVO-600 NMR spectrometers. The chemical shift (δ) values are given in ppm with TMS as internal standard, and coupling constants (J) are in Hz. EIMS and HREIMS spectra were recorded on Finnigan MAT-95 mass spectrometer. ESIMS and HRESIMS spectra were recorded on Micromass LC-MS-MS mass spectrometer. Column chromatographic separations were carried out by using silica gel H60 (300–400 mesh, Qingdao Haiyang Chemical Group Corporation), MCI GEL CHP20P (75–150 μ m, Mitsubishi Chemical Industries), and Sephadex LH-20 (Pharmacia Biotech AB) as packing materials. HSGF254 silica gel TLC plates (Yantai Chemical Industrial Institute) were used for analytical TLC. The Analytical HPLC system was composed of Waters 2690 separations module, Waters 996 diode array detector (Waters), and All-tech 2000 ELSD. A LinChrospher 100 RP-18e (Merck) column (125 \times 4 mm i.d.; particle size 5 μ m) was used for the separation. The Preparative HPLC system composed of two PrepStar SD-1 solvent delivery modules, a ProStar UV-Vis 320 detector, and a ProStar 701 Fraction Collector (Varian). A LinChrospher 100 RP-18 (Merck) column (220 \times 25 mm i.d.; particle size 12 μ m) was used for isolation. Gas chromatography was carried out on a Shimadzu GC 14-BPF apparatus equipped with a 5% OV225/AW-DMCS-Chromosorb W (80–100 mesh) column (2.5 m \times 3 mm) as well as a hydrogen-flame ionization detector.

Plant Materials

Fruits were purchased from a cultivation plant in Guangxi Province. Representative samples were deposited at the Herbarium of Shanghai Institute of Materia Medica, Chinese Academy of Sciences, China.

Extraction and Isolation

The freeze-dried fruit powder (75 kg) was extracted by maceration with 80% EtOH. After filtration and evaporation of the solvent under reduced pressure, the alcohol extract was partitioned successively with CH_2Cl_2 and n -BuOH. The n -BuOH-soluble extract (800 g) was subjected to macroporous resin column chromatography eluting with H_2O , 25% EtOH, 60% EtOH, and 95%

EtOH to yield four fractions: KG5 (600 g), KG6 (59 g), KG7 (50 g), and KG8 (30 g). KG8 was subjected to normal phase silica gel column chromatography with gradient elution [$CHCl_3$ -MeOH- H_2O 40:3:1 low layer (10 l), $CHCl_3$ -MeOH- H_2O 20:3:1 low layer (10 l), $CHCl_3$ -MeOH- H_2O 10:3:1 low layer (10 l), $CHCl_3$ -MeOH- H_2O 8:3:1 low layer (8 l), $CHCl_3$ -MeOH- H_2O 65:35:10 low layer (6 l)] to give six fractions (Fr1–6). Compound 1 (150 mg), compound 2 (80 mg), and compound 7 (150 mg) from Fr6 (5.5 g) were purified by repeated column chromatography over MCI gel, silica gel, and Sephadex LH-20, respectively. Further fractionation of KG7 by normal phase silica gel column chromatography with gradient elution [$CHCl_3$ -MeOH- H_2O 20:3:1 low layer (10 l), $CHCl_3$ -MeOH- H_2O 10:3:1 low layer (10 l), $CHCl_3$ -MeOH- H_2O 8:3:1 low layer (8 l), $CHCl_3$ -MeOH- H_2O 65:35:10 low layer (10 l), $CHCl_3$ -MeOH- H_2O 6:4:1 (6 l)] gave six fractions (Fr7–12). Compound 5 (160 mg) and compound 6 (220 mg) from Fr11 (6.5 g) were isolated by repeated column chromatography over MCI gel, silica gel and Sephadex LH-20. Compound 3 (18 mg) from Fr8 (6.5 g) were separated by repeated column chromatography over MCI gel, silica gel, Sephadex LH-20, and preparative HPLC (MeOH- H_2O , 60:40-85:15). Momordicosides A (350 mg) and B (250 mg) from Fr9 (4.3 g) were isolated by repeated normal phase silica gel.

Acid Hydrolysis of Compounds 1, 2, 3, 5, 6, and 7

Compound 1 (100 mg) in 2% HCl-dioxane (1:1, 25 ml) were heated at 40°C for 7 days in a water bath. The reaction mixtures were neutralized with Ag_2CO_3 , filtered, and then extracted with $CHCl_3$. Aglycone 4 (25 mg) was obtained from $CHCl_3$ layer by column chromatography and crystallized in MeOH. Compounds 2, 3, 5, 6, and 7 (3 mg each) were refluxed with 2% HCl-dioxane (1:1, 25 ml) at 90°C for 4 hr. The reaction mixtures were neutralized with Ag_2CO_3 , filtered, and then extracted with $CHCl_3$. The aqueous layer was evaporated, and then the residue was treated with L-cysteine methyl ester hydrochloride (4 mg) in pyridine (0.5 ml) at 60°C for 1 hr. After reaction, the solution was treated with acetic anhydride (3 ml) at 60°C for 1 hr. Authentic samples were prepared by the same procedure. The acetate derivatives were subjected to GC analysis to identify the sugars (column temperature 210°C; injection temperature 250°C; carrier gas N_2 at a flow rate of 25 ml/min). D-allose (t_R 5.0 min) was observed from 1 and 3; D-glucose (t_R 1.8 min) was observed from 2, 3, 5, 6 and 7; D-xylose (t_R 4.0 min) was observed from 6.

Enzymatic Hydrolysis of Compound 5

Compound 5 (60 mg) and momordicoside A (40 mg) were treated with cellulose in 0.1 M acetate buffer solution at 37°C for 7 days. The reaction mixtures were then extracted with $CHCl_3$. Aglycone 8 was obtained from both $CHCl_3$ layers by preparative TLC.

Spectroscopic Data of Compounds

2, 3, 5, 6, 7

Momordicoside Q (2)

Amorphous powder; $[\alpha]_D^{25} = -76$ (c 0.1600, MeOH); IR ν_{max} (KBr) 3396, 3165, 2935, 2783, 1612, 1514, 1454, 1417, 1277, 1263, 1223, 1165, 1122, 1039, 814, 689 cm^{-1} ; 1H NMR and ^{13}C NMR data see Table 1; HRESIMS m/z 675.4113 (calcd for $C_{36}H_{60}O_{10}Na$ $[M+Na]^+$, 675. 4084).

Momordicoside R (3)

Amorphous powder; $[\alpha]_D^{23} = -64$ (c 0.188, MeOH); IR ν_{\max} (KBr) 3415, 2928, 2874, 1643, 1466, 1377, 1155, 1082, 1032 cm^{-1} ; ^1H NMR and ^{13}C NMR data see Table 1; HRESIMS m/z 6837.4632 (calcd for $\text{C}_{42}\text{H}_{70}\text{O}_{15}\text{Na}$ $[\text{M}+\text{Na}]^+$, 837.4612).

Momordicoside S (5)

Amorphous powder; $[\alpha]_D^{23} = -8$ (c 0.2245, MeOH); IR ν_{\max} (KBr) 3406, 2933, 2873, 1646, 1551, 1452, 1383, 1306, 1076, 1038, 534; ^1H NMR and ^{13}C NMR data see Table 1; HRESIMS m/z 1001.5253 (calcd for $\text{C}_{48}\text{H}_{82}\text{O}_{20}\text{Na}$ $[\text{M}+\text{Na}]^+$, 1001.5297).

Momordicoside T (6)

Amorphous powder; $[\alpha]_D^{23} = -1$ (c 0.1385, MeOH); IR ν_{\max} (KBr) 3408, 2931, 2857, 1639, 1468, 1381, 1308, 1163, 1076, 1039 cm^{-1} ; ^1H NMR and ^{13}C NMR data see Table 1; HRESIMS m/z 1113.5714 (calcd for $\text{C}_{53}\text{H}_{90}\text{O}_{24}\text{Na}$ $[\text{M}+\text{Na}]^+$, 1113.5720).

Momorcharaside B (7)

Amorphous powder; $[\alpha]_D^{23} = -20$ (c 0.1600, MeOH); IR ν_{\max} (KBr) 3406, 2949, 2875, 1633, 1468, 1381, 1167, 1076, 1036, 951, 619 cm^{-1} ; ^1H NMR and ^{13}C NMR data see Table 1; HRESIMS m/z 677.4224 (calcd for $\text{C}_{36}\text{H}_{62}\text{O}_{10}\text{Na}$ $[\text{M}+\text{Na}]^+$, 677.4241).

X-Ray Crystallographic Data for Compound 4

$\text{C}_{30}\text{H}_{56}\text{O}_8 + 3 \text{H}_2\text{O}$, mol. wt. = 544.75, orthorhombic space group $P2_12_12_1$, $a = 6.33550(12) \text{ \AA}$, $b = 13.7125(2) \text{ \AA}$, $c = 35.1964(7) \text{ \AA}$, $V = 3057.71(18) \text{ \AA}^3$, $Z = 4$, $d = 1.183 \text{ g/cm}^3$. $F(000) = 1200$, $\mu = 0.676 \text{ mm}^{-1}$. A single crystal of dimensions $0.12 \times 0.03 \times 0.02 \text{ mm}$ was used for X-ray measurements. The data collection was performed on a Gemini R Ultra diffractometer using $\text{Cu-K}\alpha$ -radiation. Data were collected up to $\theta = 65.60^\circ$ at 100 K. A total of 5059, thereof 4908, independent reflections were measured, giving a R_{int} of 0.0312. Programs used were Data collection and reduction Crysalis Version 1.171.35. Crystal structure solution and refinement was achieved using direct methods as implemented in SHELXTL Version 6.12 and visualized using XP program. 359 Parameters were refined using 4908 reflections with $F_0 > 4\sigma$ (F_c) giving $R_1 = 0.0469$, $wR_2 = 0.1050$, Goodness of Fit 1.144, remaining electron density 0.247 and $-0.217 \text{ e}^- \text{ \AA}^{-3}$. The absolute structure could be determined with high probability giving a Flack \times Parameter of $-0.0505(0.2077)$, the result is confirmed by the analysis of Bijvoet pairs implemented in Platon. CCDC 654600 contains the supplementary crystallographic data for this paper. These data can be obtained free of charge via <http://www.ccdc.cam.ac.uk/conts/retrieving.html> (or from the CCDC, 12 Union Road; Cambridge CB2 1EZ, UK; fax: +44 1223 336 033; email: deposit@ccdc.cam.ac.uk).

Cell Culture

L6 myoblasts up to passage 15 were cultured in α -minimal essential medium (α -MEM) supplemented with 10% heat-inactivated fetal calf serum (FCS) at 37°C in 5% CO_2 . For differentiation into myotubes, cells were cultured in α -MEM supplemented with 2% heat-inactivated FCS at 37°C in 5% CO_2 and were maintained in this medium postdifferentiation. Myotubes were used for experiments 5–7 days after differentiation. 3T3-L1 cells were cultured at 37°C in Dulbecco's modified Eagle's medium (DMEM) containing 10% bovine calf serum (BCS) in an atmosphere of 10% CO_2 . The differentiation of 3T3-L1 cells was induced as described previously (Govers et al., 2004). Briefly, the confluent cells were incubated for 2 days in DMEM that was supplemented with 10% fetal bovine serum (FBS), 0.5 mM 3-isobutyl-1-methylxanthine, 1 μM dexamethasone, and 5 $\mu\text{g}/\text{ml}$ insulin. Thereafter, the medium was replaced every other day with DMEM containing 10% FBS and 5 $\mu\text{g}/\text{ml}$ insulin.

GLUT4 Translocation Assay

HA-GLUT4 translocation to the PM was measured as previously described (Govers et al., 2004) with minor modifications. Briefly, cells were grown in black, clear-bottom, 96-well plates and starved for 2 hr in serum- and bicarbonate-free DMEM containing 20 mM HEPES (pH 7.4) and 0.2% BSA (DMEM/BSA) at 37°C before starting the experiment. Plates were then transferred to 19°C , and vehicle, 100 nM insulin, 2 mM AICAR, 10 μM wortmannin, or test compounds were added for 30 min. At given time points, paraformaldehyde was added to the wells to a concentration of 3%. After 15 min, the paraformaldehyde was quenched by the addition of glycine (final concentration, 50 mM). The cells were washed extensively and incubated for 20 min with 5% normal

swine serum (NSS) in the absence or presence of 0.1% saponin to analyze the amount of HA-GLUT4 at the PM or the total HA-GLUT4 content, respectively. Cells were incubated for 60 min with anti-HA or, as a control, a nonrelevant antibody (mouse IgG1-MOPC21) in PBS containing 2% NSS. Cells were extensively washed and incubated for 20 min in 5% NSS in the presence or absence of 0.1% saponin. Cells were then incubated with ALEXA488-conjugated goat-antimouse in PBS containing 2% NSS. After washing, fluorescence was measured using the bottom-reading mode in a fluorescence microtiter plate reader (FLUOstar Galaxy, BMG Labtechnologies).

Determination of Phosphorylation of Akt and AMPK

Differentiated 3T3-L1 and L6 cells were serum-starved in DMEM/BSA (2 hr at 37°C) prior to incubation either with test compounds (1, 4, 5, 8) or vehicle (DMSO containing saline, final concentration of DMSO: 0.2%) for 30 min, or with 100 nM Insulin or 2 mM AICAR for 25 min. Following treatment, cells were washed three times with ice-cold PBS and subsequently lysed in $1 \times$ RIPA buffer (50 mM Tris HCl [pH 8], 150 mM NaCl, 1% NP-40, 0.5% sodium Deoxycholate, 0.1% SDS) supplemented with Complete protease inhibitor cocktail (Roche) and phosphatase inhibitors [2 mM Na_3VO_4 , 1 mM $\text{Na}_4\text{P}_2\text{O}_7$, 1 mM $(\text{NH}_4)_6\text{Mo}_7\text{O}_{24} \cdot 4\text{H}_2\text{O}$, 10 mM NaF], then passed through a 22-gauge needle $10 \times$ and centrifuged at $20,000 \times g$ for 20 min. Supernatant protein concentration was determined via BCA assay (Pierce). Equal amounts of protein were then diluted $4 \times$ in SDS sample buffer (62.5 mM Tris-HCl, 20% glycerol, 2% SDS, 75 μM DTT, and 0.05% bromophenol blue), subjected to SDS PAGE and immunoblotted with antibodies specific for Akt, phospho-Akt (Ser473), AMPK, and phospho-AMPK- α (Thr172) (Cell Signaling Technology). Immunoblots were quantified using Image J software (NIH) and expressed at a ratio of phosphorylation to total.

Experimental Animals

C57BL/6 mice (10 week old males) supplied by the Animal Resources Center (Perth, Australia) were acclimatized in communal cages at 22°C , with a 12 hr light, 12 hr dark cycle (lights on at 0700) for 1 week and had access to a standard chow diet (Gordon's Specialty Stock Feed) or a high (lard) fat diet for 7 weeks ad libitum to generate glucose intolerance similarly to a previous report (Iglesias et al., 2002). All experimental procedures were approved by the Garvan Institute Animal Experimentation Ethics Committee, following guidelines issued by the National Health and Medical Research Council of Australia.

Determination of Whole-Body Energy Expenditure and Fat Oxidation

The oxygen consumption rate (VO_2) and CO_2 production rate was measured using an eight chamber indirect calorimeter (Oxymax series; Columbus Instruments) as described previously (Molero et al., 2006). The animals were placed in the metabolic chamber (20 cm \times 10 cm \times 12.5 cm) at 9:30 a.m. After 2 hr of acclimation, momordicoside S (5) (100 mg/kg), AICAR (250 mg/kg) or normal saline (vehicle) was injected subcutaneously. VO_2 was measured in individual mice at 27 min intervals over a 24 hr period under a consistent environmental temperature (22°C) and its values are proportional to energy expenditure. During the study, mice had ad libitum access to food and water. Respiratory exchange rate (RER) was calculated from VO_2 and CO_2 production and its values are in reverse proportion to whole-body fat oxidation.

Measurement of Blood Glucose and Glucose Tolerance Test

The experiment was performed in mice after 5–7 hr of fasting. Blood glucose taken from the tail tip was measured using a glucometer (Accu-Chek, Roche). Following the measurement of basal blood glucose concentration at 0 min, vehicle solution (100 μl of 15% glycerol, 5% ethanol, and 80% saline), momordicoside S (5) (100 mg/kg), momordicoside T (6) (at a low dose: 10 mg/kg), AICAR (500 mg/kg), or metformin (200 mg/kg) was injected into the peritoneal cavity. Around 60 min, a sample was taken to assess the direct effect on blood glucose and this was immediately followed by an intraperitoneal glucose tolerance test (ipGTT). The glucose load was 3.0 g/kg for normal, chow-fed mice and 2.0 g/kg for insulin-resistant, high-fat-fed mice. These different glucose doses for different insulin sensitivity states were chosen to maximize the detection of treatment effects based on pilot experiments.

Data Analyses

An unpaired student t test was used for the comparison between treatments or groups and a p value ≤ 0.05 is considered statistically significant.

SUPPLEMENTAL DATA

Supplemental Data include NMR data of compounds **1-10** and UPLC/MS analyses of bitter melon extracts and can be found with this article online at <http://www.chembiol.com/cgi/content/full/15/3/263/DC1/>.

ACKNOWLEDGMENTS

This study was supported by the National Natural Science Foundation of China (grant 30770236 to Y.Y.) and the National Health and Medical Research Council of Australia (NHMRC) (grant 481334 to J.-M.Y.). Financial support from the Ministry of Science and Technology of China (2004CB518902) was also greatly acknowledged. J.-M.Y. and C.H.-B. were supported by Australian International Linkage Program and Diabetes Australia Research Trust. A.R. was supported by an Australian APA scholarship. N.T. is a NHMRC Peter Doherty Postdoctoral Fellow and D.E.J. is a NHMRC Senior Principal Research Fellow.

Received: September 18, 2007

Revised: January 21, 2008

Accepted: January 31, 2008

Published: March 21, 2008

REFERENCES

- Brunmair, B., Staniek, K., Gras, F., Scharf, N., Althaym, A., Clara, R., Roden, M., Gnaiger, E., Nohl, H., Waldhäusl, W., et al. (2004). Thiazolidinediones, like metformin, inhibit respiratory complex I: a common mechanism contributing to their antidiabetic actions? *Diabetes* **53**, 1052–1059.
- Govers, R., Coster, A.C., and James, D.E. (2004). Insulin increases cell surface GLUT4 levels by dose dependently discharging GLUT4 into a cell surface recycling pathway. *Mol. Cell. Biol.* **24**, 6456–6466.
- Grover, J.K., and Yadav, S.P. (2004). Pharmacological actions and potential uses of *Momordica charantia*: a review. *J. Ethnopharmacol.* **93**, 123–132.
- Harinantenaina, L., Tanaka, M., Takaoka, S., Oda, M., Mogami, O., Uchida, M., and Asakawa, Y. (2006). *Momordica charantia* constituents and antidiabetic screening of the isolated major compounds. *Chem. Pharm. Bull. (Tokyo)* **54**, 1017–1021.
- Huang, S., and Czech, M.P. (2007). The GLUT4 glucose transporter. *Cell Metab.* **5**, 237–252.
- Iglesias, M.A., Ye, J.M., Frangioudakis, G., Saha, A.K., Tomas, E., Ruderman, N.B., Cooney, G.J., and Kraegen, E.W. (2002). AICAR administration causes an apparent enhancement of muscle and liver insulin action in insulin-resistant high-fat-fed rats. *Diabetes* **51**, 2886–2894.
- Khanna, P., Jain, S.C., Panagariya, A., and Dixit, V.P. (1981). Hypoglycemic activity of polypeptide from a plant source. *J. Nat. Prod.* **44**, 648–655.
- Koehn, F.E., and Carter, G.T. (2005). The evolving role of natural products in drug discovery. *Nat. Rev. Drug Discov.* **4**, 206–220.
- Lee, Y.S., Kim, W.S., Kim, K.H., Yoon, M.J., Cho, H.J., Shen, Y., Ye, J.M., Lee, C.H., Oh, W.K., Kim, C.T., et al. (2006). Berberine, a natural plant product, activates AMP-activated protein kinase with beneficial metabolic effects in diabetic and insulin-resistant states. *Diabetes* **55**, 2256–2264.
- Lipinski, C.A., Lombardo, F., Dominy, B.W., and Feeney, P.J. (2001). Experimental and computational approaches to estimate solubility and permeability in drug discovery and development settings. *Adv. Drug Deliv. Rev.* **46**, 3–26.
- Matsuda, H., Nakamura, S., Murakami, T., and Yoshikawa, M. (2007). Structures of new cucurbitane-type triterpenes and glycosides, karavilagenins D and E, and karavilosides VI, VII, VIII, IX, X, and XI, from the fruit of *Momordica charantia*. *Heterocycles* **71**, 331–341.
- Meng, Z., Zhang, H., Zhao, Y., Lan, J., and Du, L. (2007). Transport behavior and efflux of Rg1 in rat pulmonary epithelial cells. *Biomed. Chromatogr.* **21**, 635–641.
- Miyahara, Y., Okabe, H., and Yamauchi, T. (1981). Studies on the constituents of *Momordica charantia* L. II. Isolation and characterization of minor seed glycosides, Momordicosides C, D and E. *Chem. Pharm. Bull. (Tokyo)* **29**, 1561–1566.
- Molero, J.C., Turner, N., Thien, C.B., Langdon, W.Y., James, D.E., and Cooney, G.J. (2006). Genetic ablation of the c-Cbl ubiquitin ligase domain results in increased energy expenditure and improved insulin action. *Diabetes* **55**, 3411–3417.
- Moller, D.E. (2001). New drug targets for type 2 diabetes and the metabolic syndrome. *Nature* **414**, 821–827.
- Murakami, T., Emoto, A., Matsuda, H., and Yoshikawa, M. (2001). Medicinal foodstuffs. XXI. Structures of new cucurbitane-type triterpene glycosides, goyaglycosides-a, -b, -c, -d, -e, -f, -g, and -h, and new oleanane-type triterpene saponins, goyasaponins I, II, and III, from the fresh fruit of Japanese *Momordica charantia* L. *Chem. Pharm. Bull. (Tokyo)* **49**, 54–63.
- Musi, N. (2006). AMP-activated protein kinase and type 2 diabetes. *Curr. Med. Chem.* **13**, 583–589.
- Nakamura, S., Murakami, T., Nakamura, J., Kobayashi, H., Matsuda, H., and Yoshikawa, M. (2006). Structures of new cucurbitane-type triterpenes and glycosides, karavilagenins and karavilosides, from the dried fruit of *Momordica charantia* L. in Sri Lanka. *Chem. Pharm. Bull. (Tokyo)* **54**, 1545–1550.
- Okabe, H., Miyahara, Y., Yamauchi, T., Miyahara, K., and Kawasaki, T. (1980). Studies on the constituents of *Momordica charantia* L. I. Isolation and characterization of momordicosides A and B, glycosides of a pentahydroxy-cucurbitane triterpene. *Chem. Pharm. Bull. (Tokyo)* **28**, 2753–2762.
- Okabe, H., Miyahara, Y., and Yamauchi, T. (1982a). Studies on the constituents of *Momordica charantia* L. III. Characterization of new cucurbitacin glycosides of the immature fruits. (1). Structures of Momordicosides G, F1, F2 and I. *Chem. Pharm. Bull. (Tokyo)* **30**, 3977–3986.
- Okabe, H., Miyahara, Y., and Yamauchi, T. (1982b). Studies on the constituents of *Momordica charantia* L. IV. Characterization of the new cucurbitacin glycosides of the immature fruits. (2). Structures of the bitter glycosides, momordicosides K and L. *Chem. Pharm. Bull. (Tokyo)* **30**, 4334–4340.
- Pereira, G.C., Branco, A.F., Matos, J.A., Pereira, S.L., Parke, D., Perkins, E.L., Serafim, T.L., Sardao, V.A., Santos, M.S., Moreno, A.J., et al. (2007). Mitochondrially targeted effects of berberine [Natural Yellow 18, 5,6-dihydro-9,10-dimethoxybenzo(g)-1,3-benzodioxolo(5,6-a) quinolinium] on K1735-M2 mouse melanoma cells: comparison with direct effects on isolated mitochondrial fractions. *J. Pharmacol. Exp. Ther.* **323**, 636–649.
- Shaw, R.J., Lamia, K.A., Vasquez, D., Koo, S.H., Bardeesy, N., Depinho, R.A., Montminy, M., and Cantley, L.C. (2005). The kinase LKB1 mediates glucose homeostasis in liver and therapeutic effects of metformin. *Science* **310**, 1642–1646.
- Smyth, S., and Heron, A. (2006). Diabetes and obesity: the twin epidemics. *Nat. Med.* **12**, 75–80.
- Ye, J.M., Ruderman, N.B., and Kraegen, E.W. (2005). AMP-activated protein kinase and malonyl-CoA: Targets for treating insulin resistance? *Drug Disc. Today: Ther. Strateg.* **2**, 157–163. doi: 10.1016/j.ddstr.2005.05.019.
- Zhou, G., Myers, R., Li, Y., Chen, Y., Shen, X., Fenyk-Melody, J., Wu, M., Ventre, J., Doebber, T., Fujii, N., et al. (2001). Role of AMP-activated protein kinase in mechanism of metformin action. *J. Clin. Invest.* **108**, 1167–1174.
- Zhu, Z.J., Zhong, Z.C., Luo, Z.Y., and Xiao, Z.Y. (1990). Studies on the active constituents of *Momordica charantia* L. *Yaoxue Xuebao* **25**, 898–903.
- Zimmet, P., Alberti, K.G., and Shaw, J. (2001). Global and social implications of the diabetic epidemic. *Nature* **414**, 782–787.

Chemistry & Biology 15

Supplemental Data

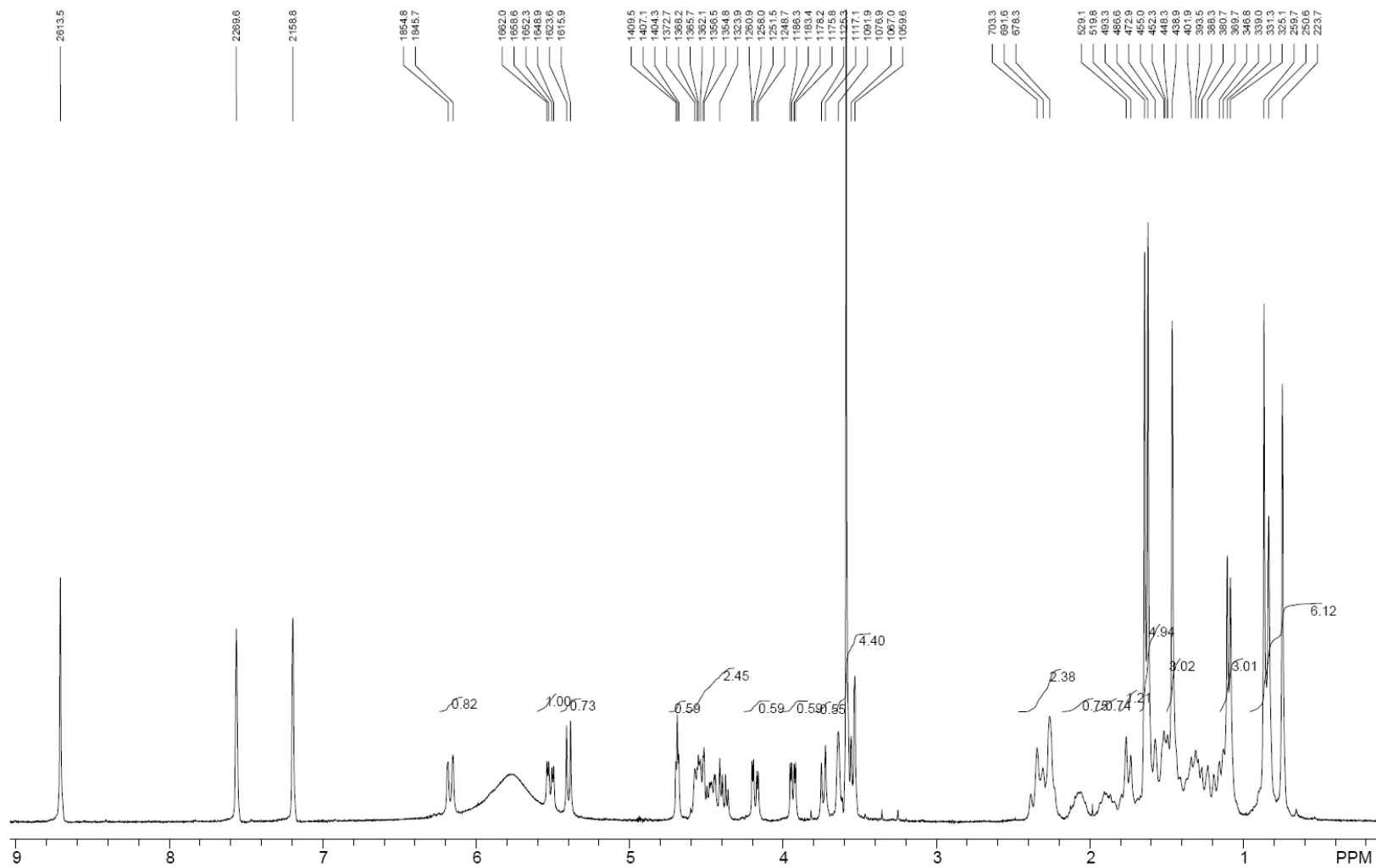
Antidiabetic Activities of Triterpenoids

Isolated from Bitter Melon Associated

with Activation of the AMPK Pathway

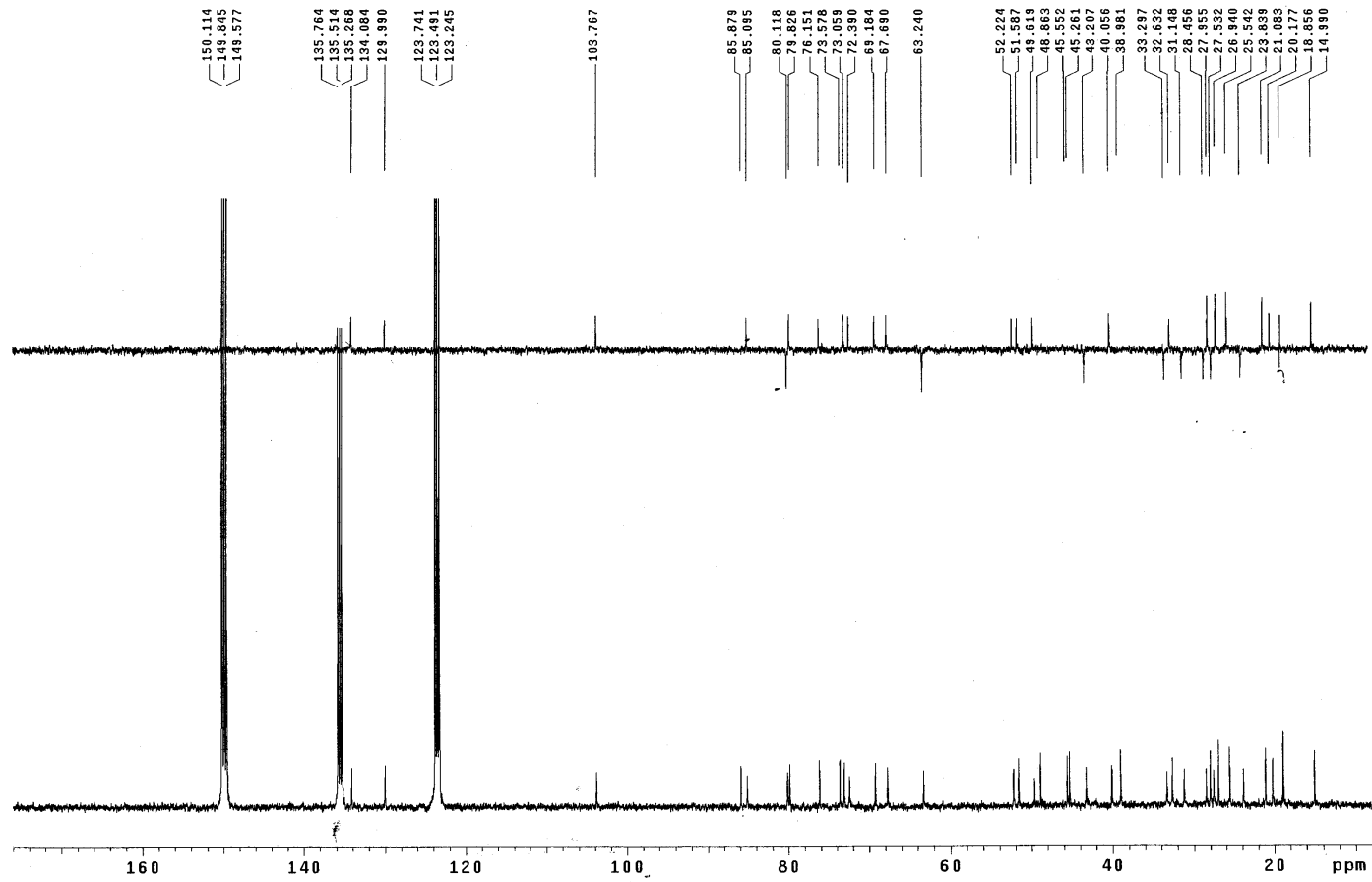
Min-Jia Tan, Ji-Ming Ye, Nigel Turner, Cordula Hohnen-Behrens, Chang-Qiang Ke, Chun-Ping Tang, Tong Chen, Hans-Christoph Weiss, Ernst-Rudolf Gesing, Alex Rowland, David E. James, and Yang Ye

¹H NMR of Compound 1

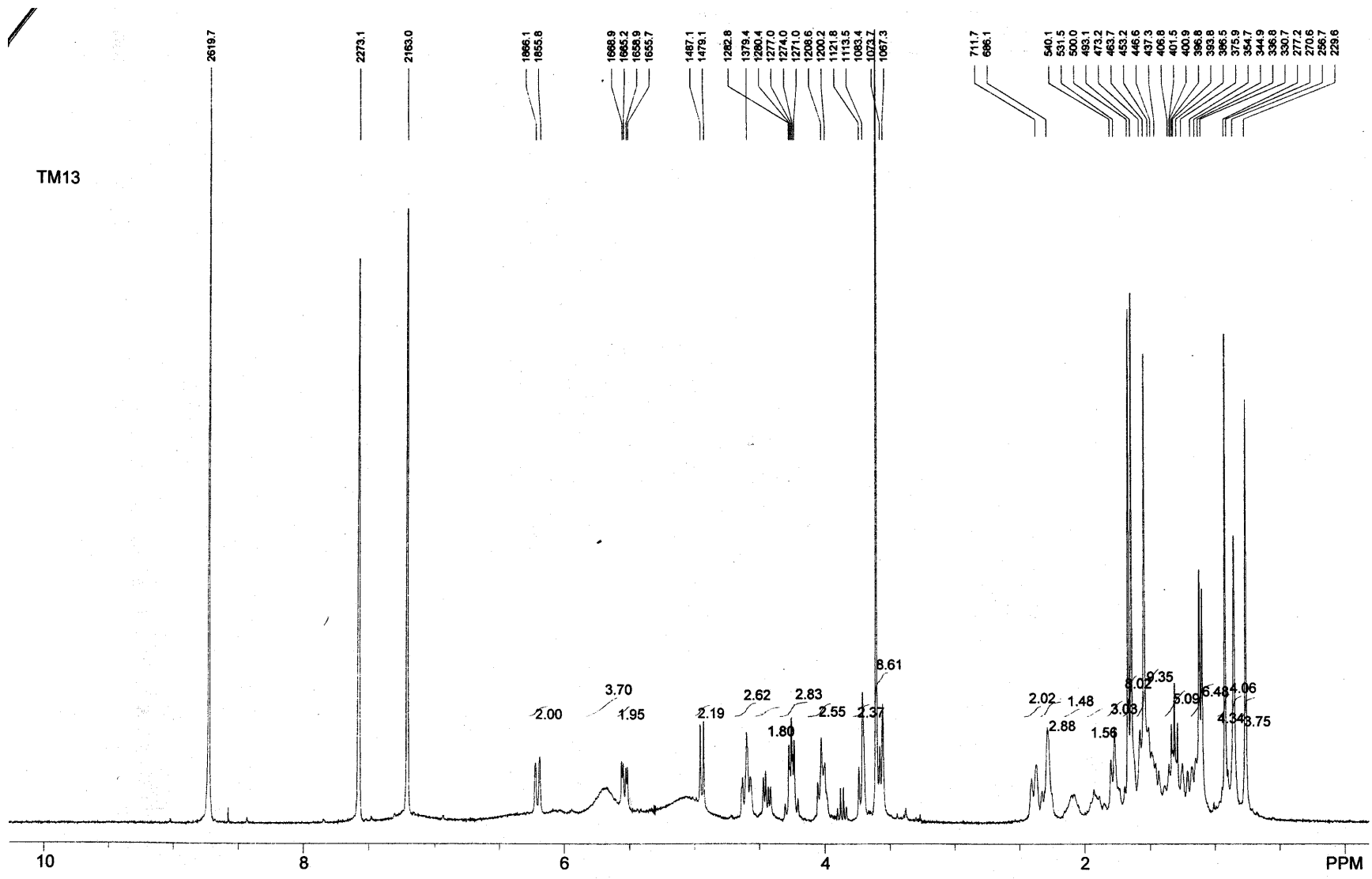


^{13}C NMR of Compound 1

TM08 C5D5N BB+DEPT-135 05-02-21

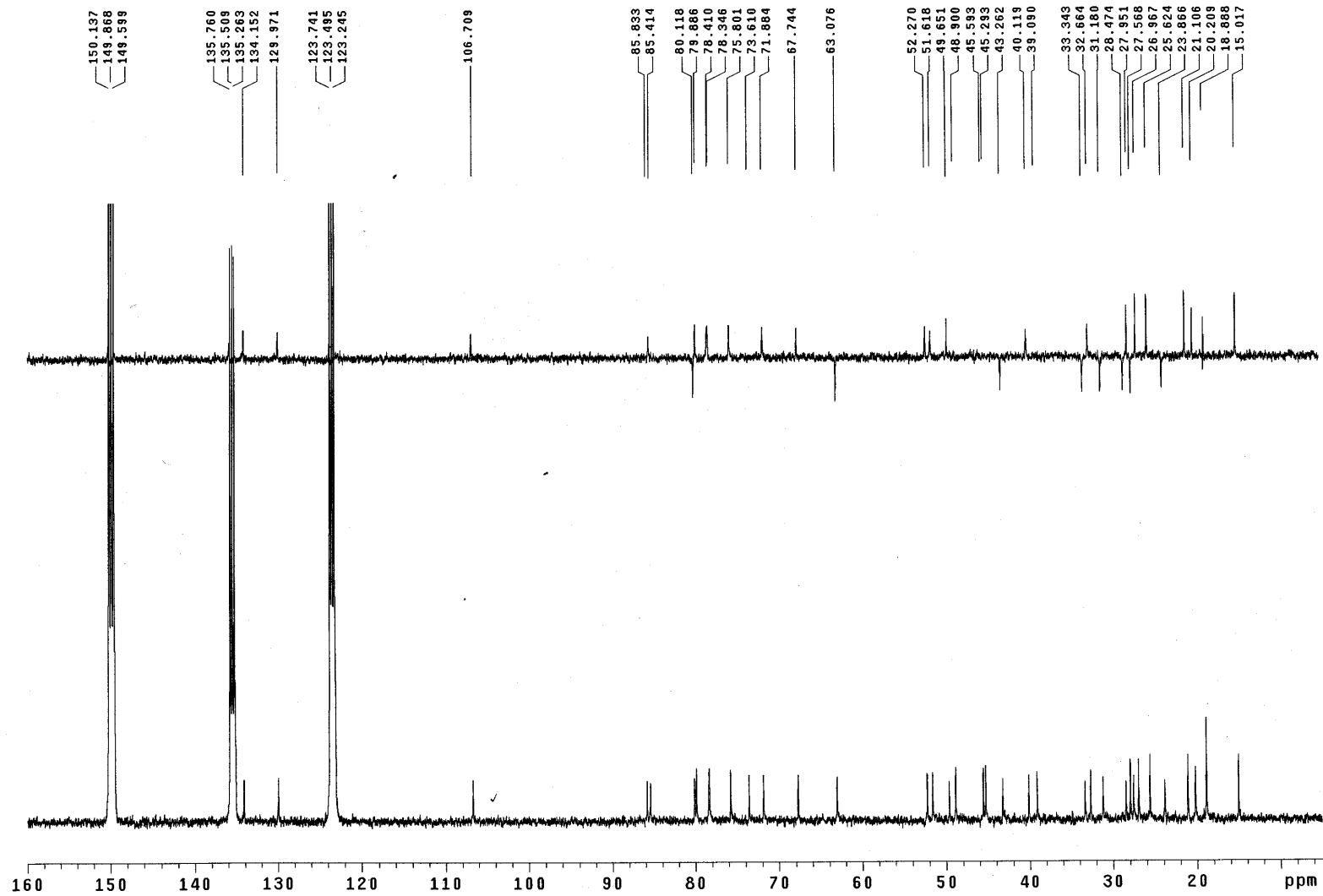


¹H NMR of Compound 2

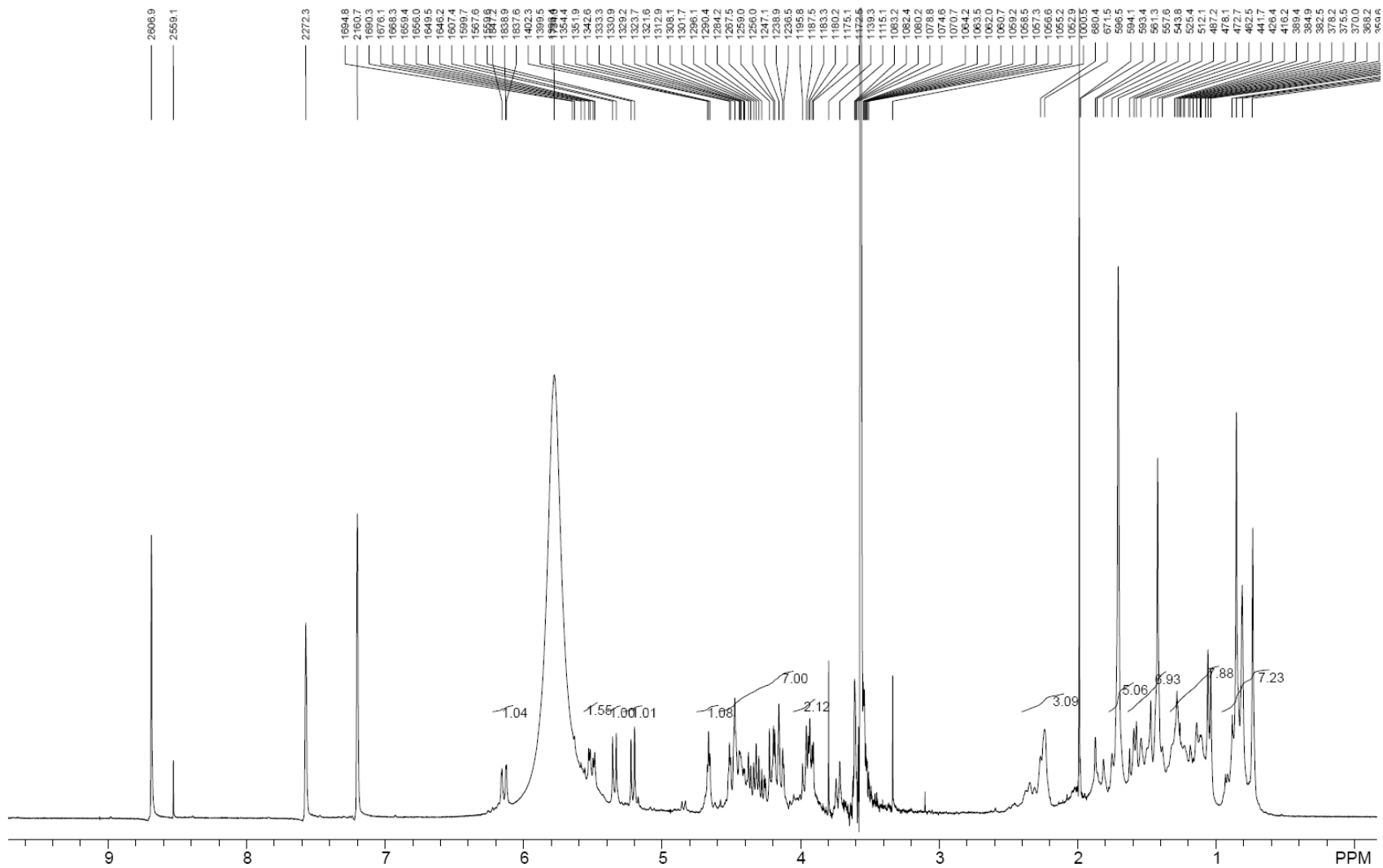


¹³C NMR of Compound 2

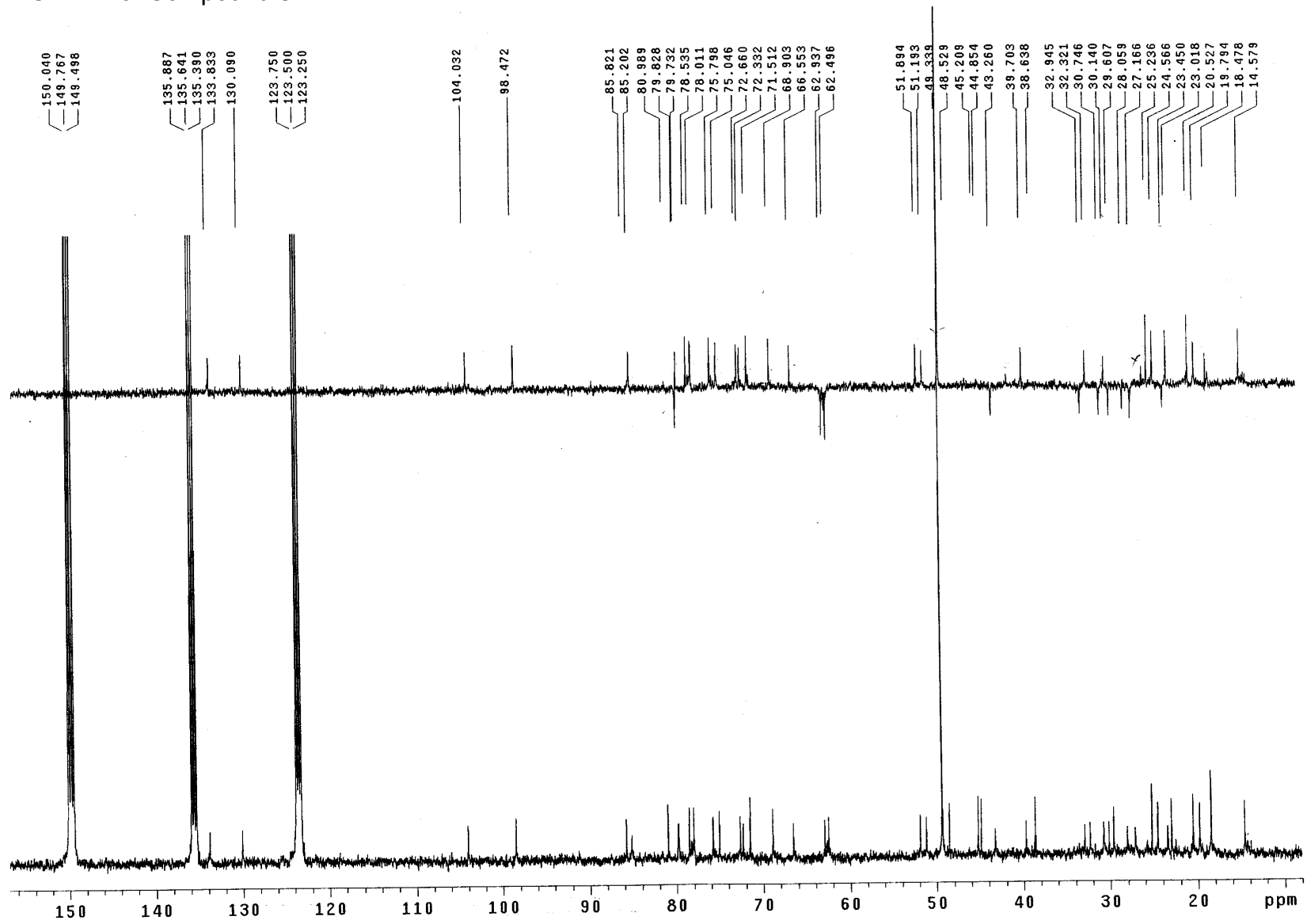
M13 C5D5N BB+DEPT-135 05-03-09



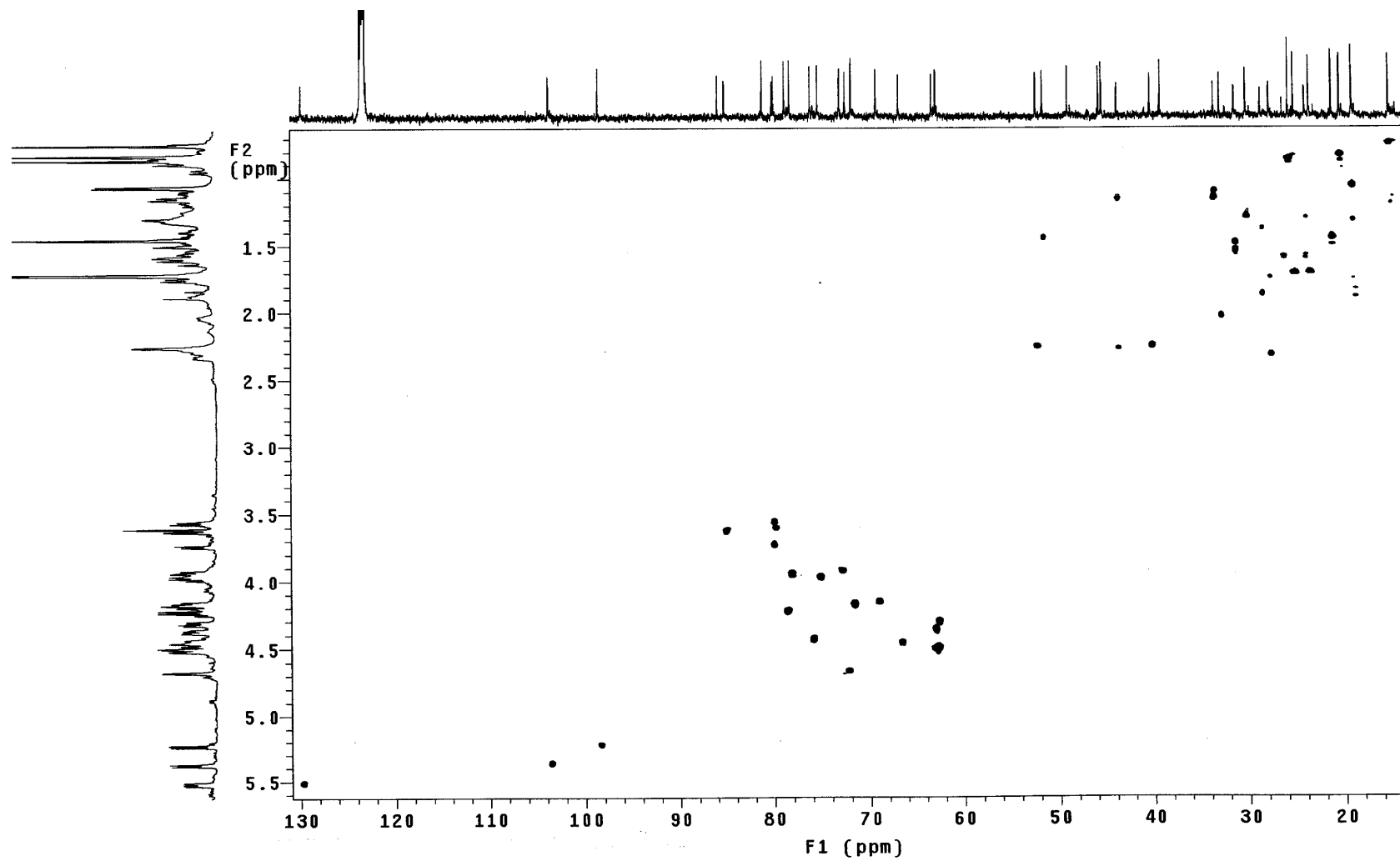
¹H NMR of Compound 3



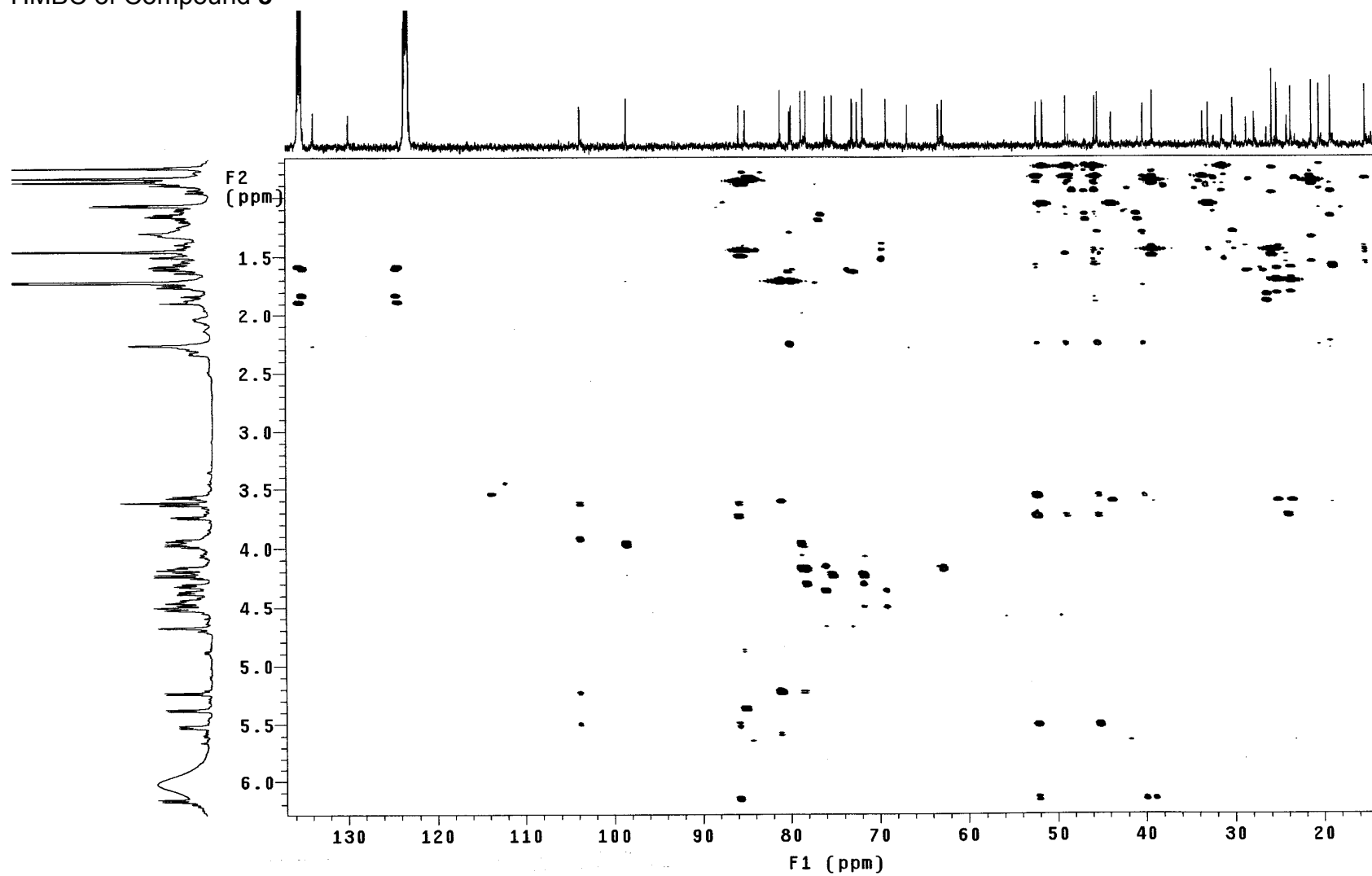
¹³C NMR of Compound 3



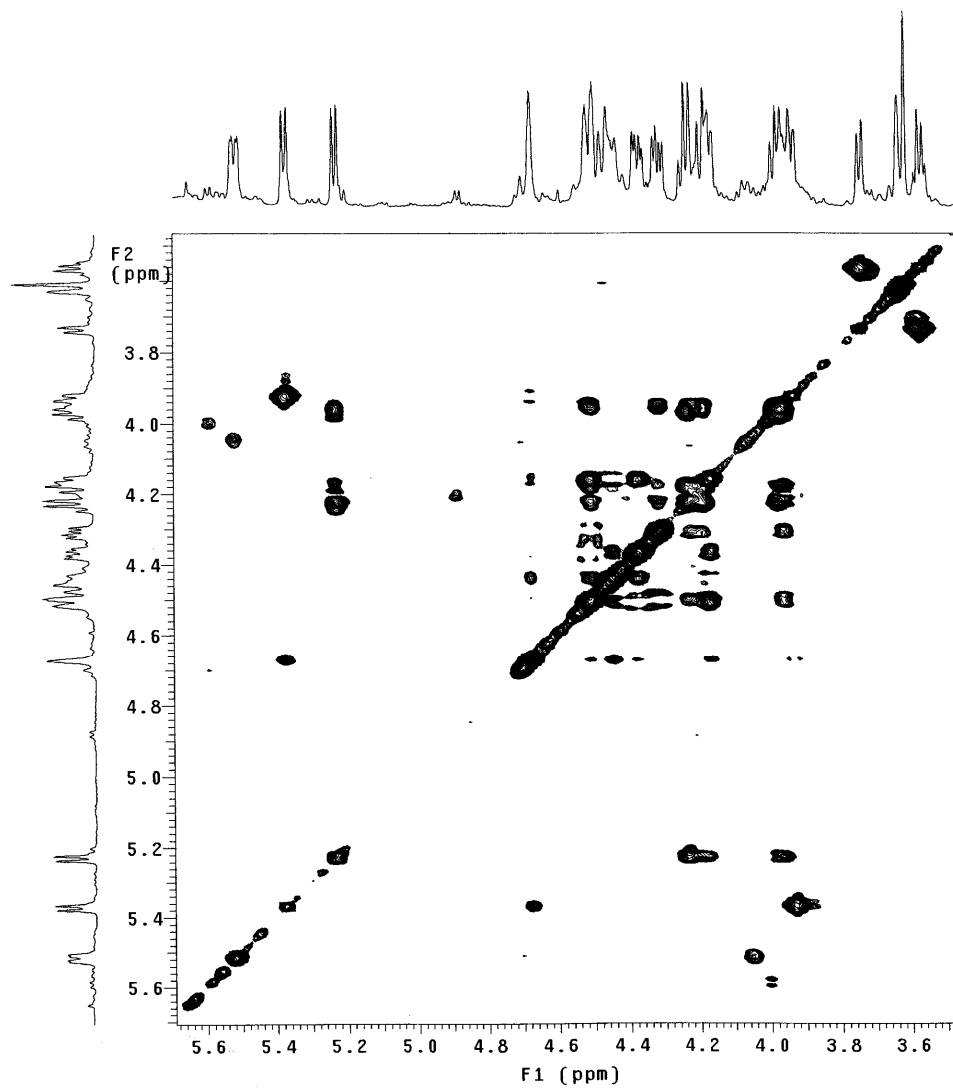
HSQC of Compound 3



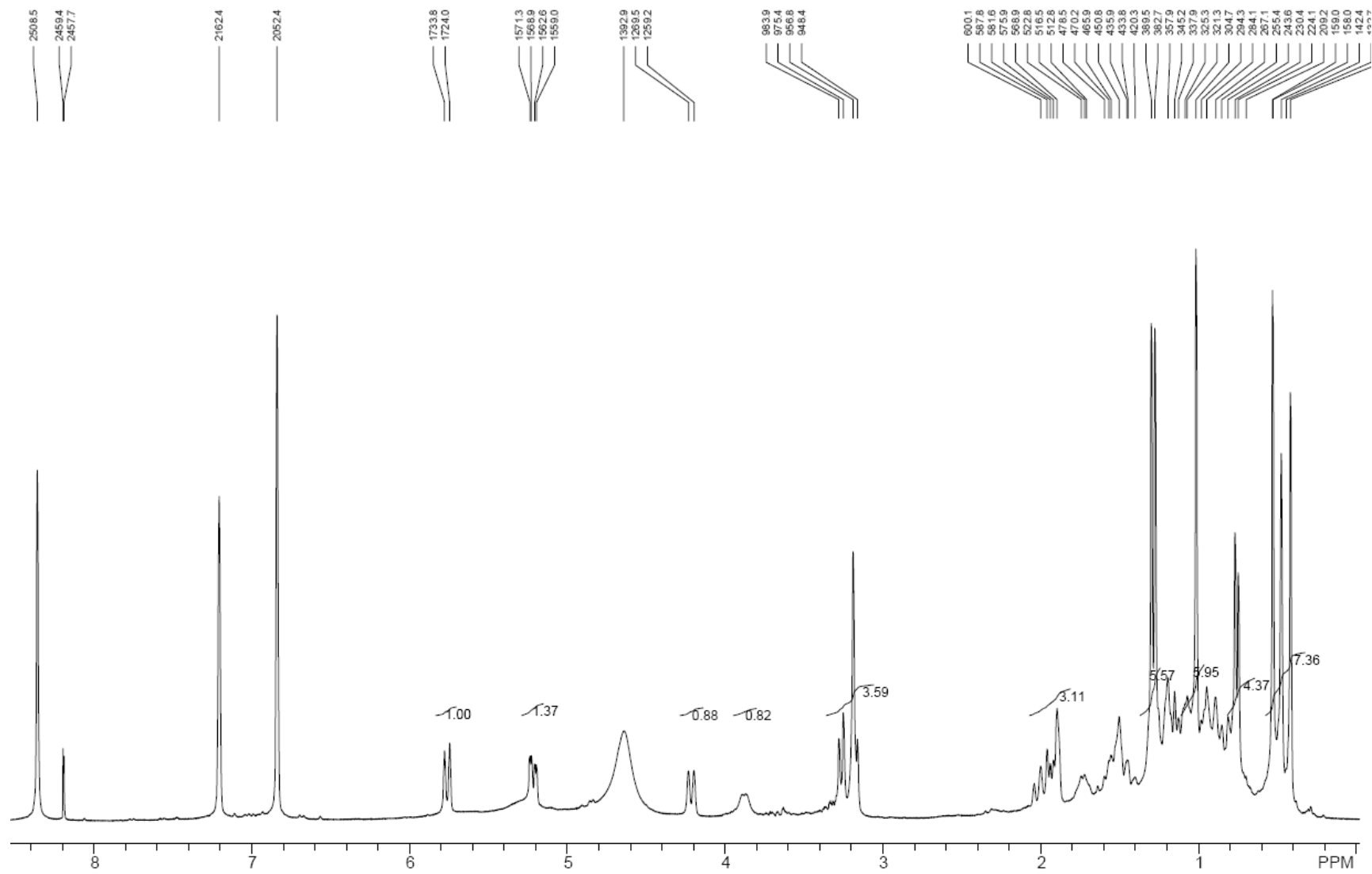
HMBC of Compound 3



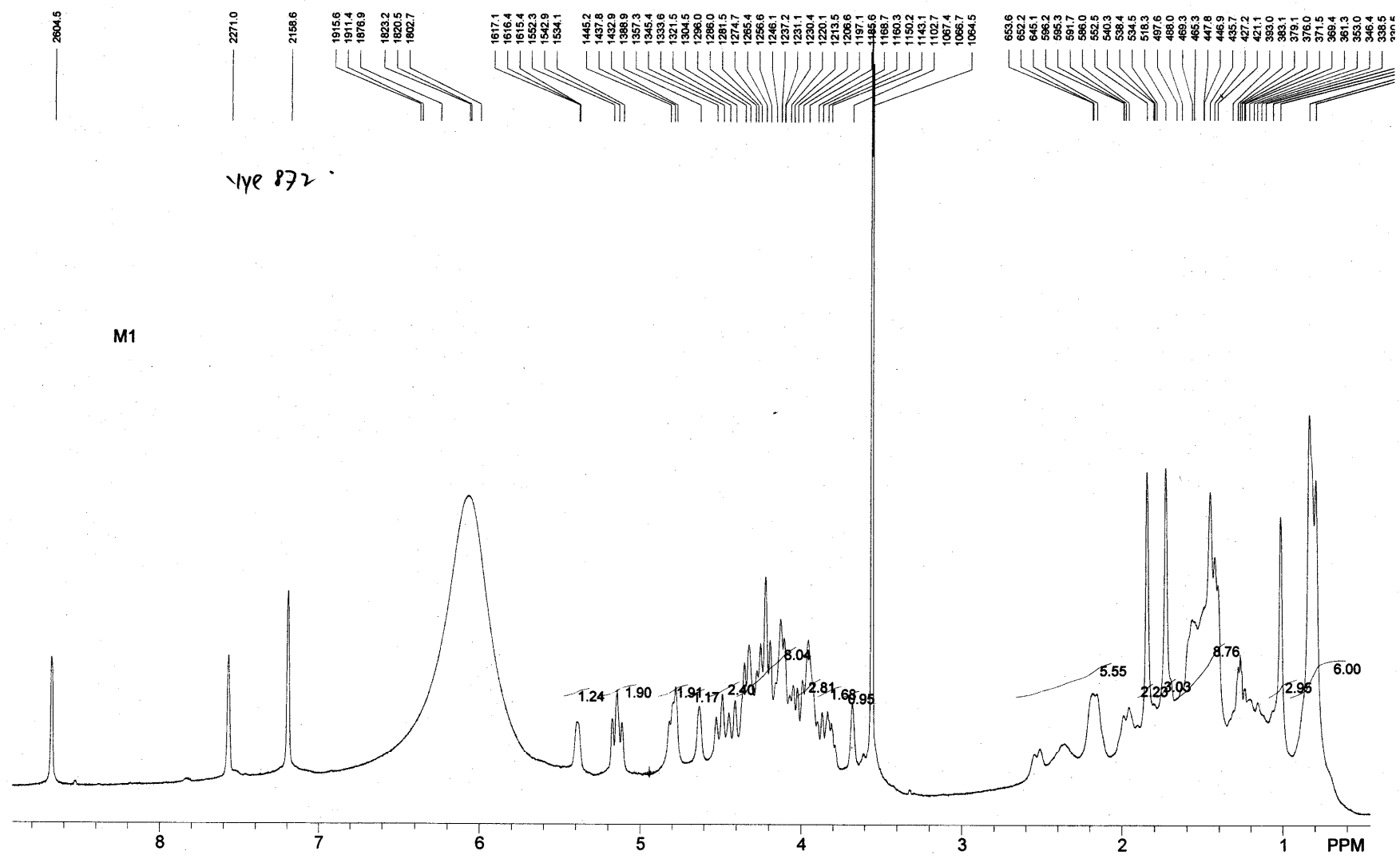
TOCSY of Compound 3



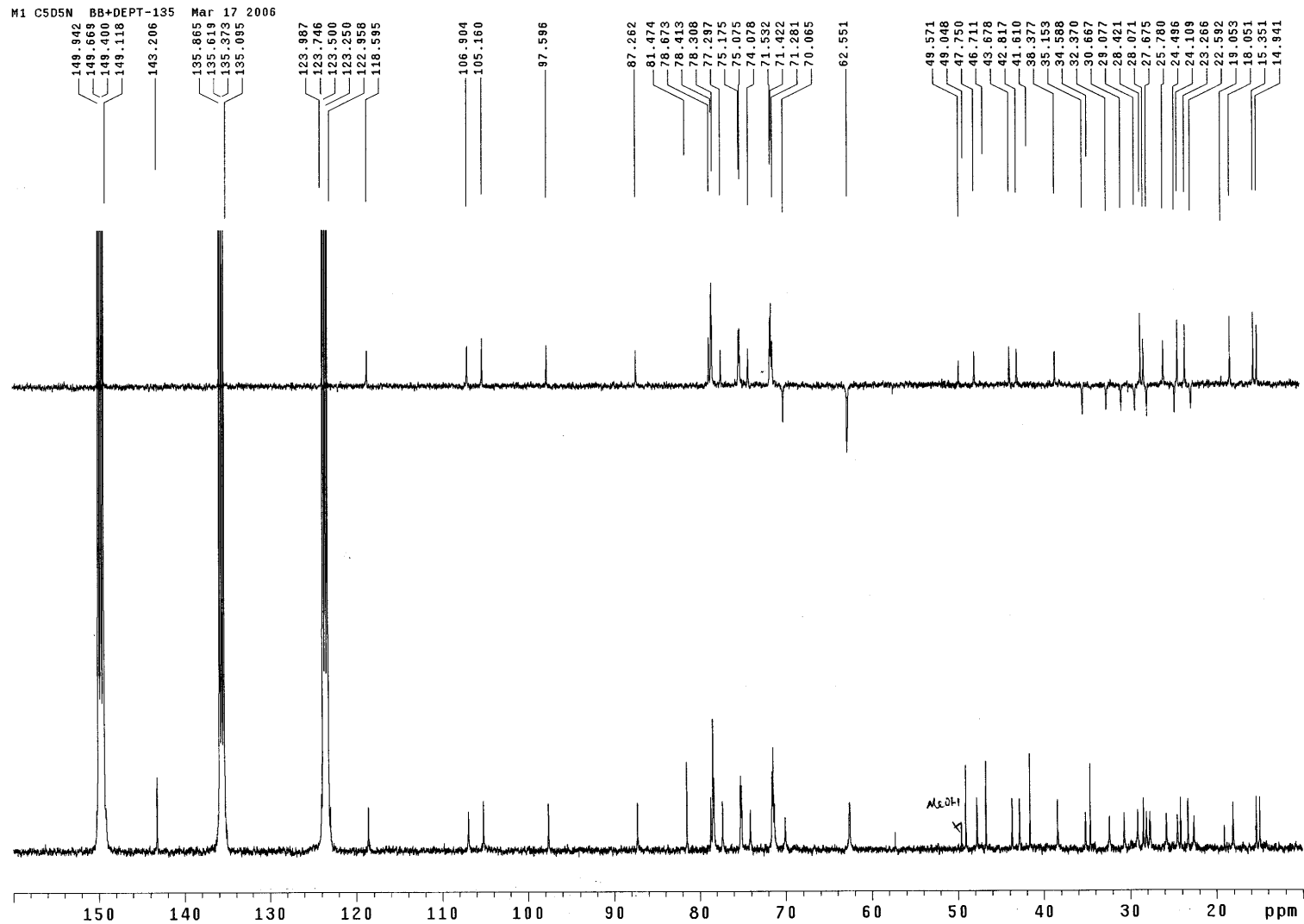
¹H NMR of Compound 4



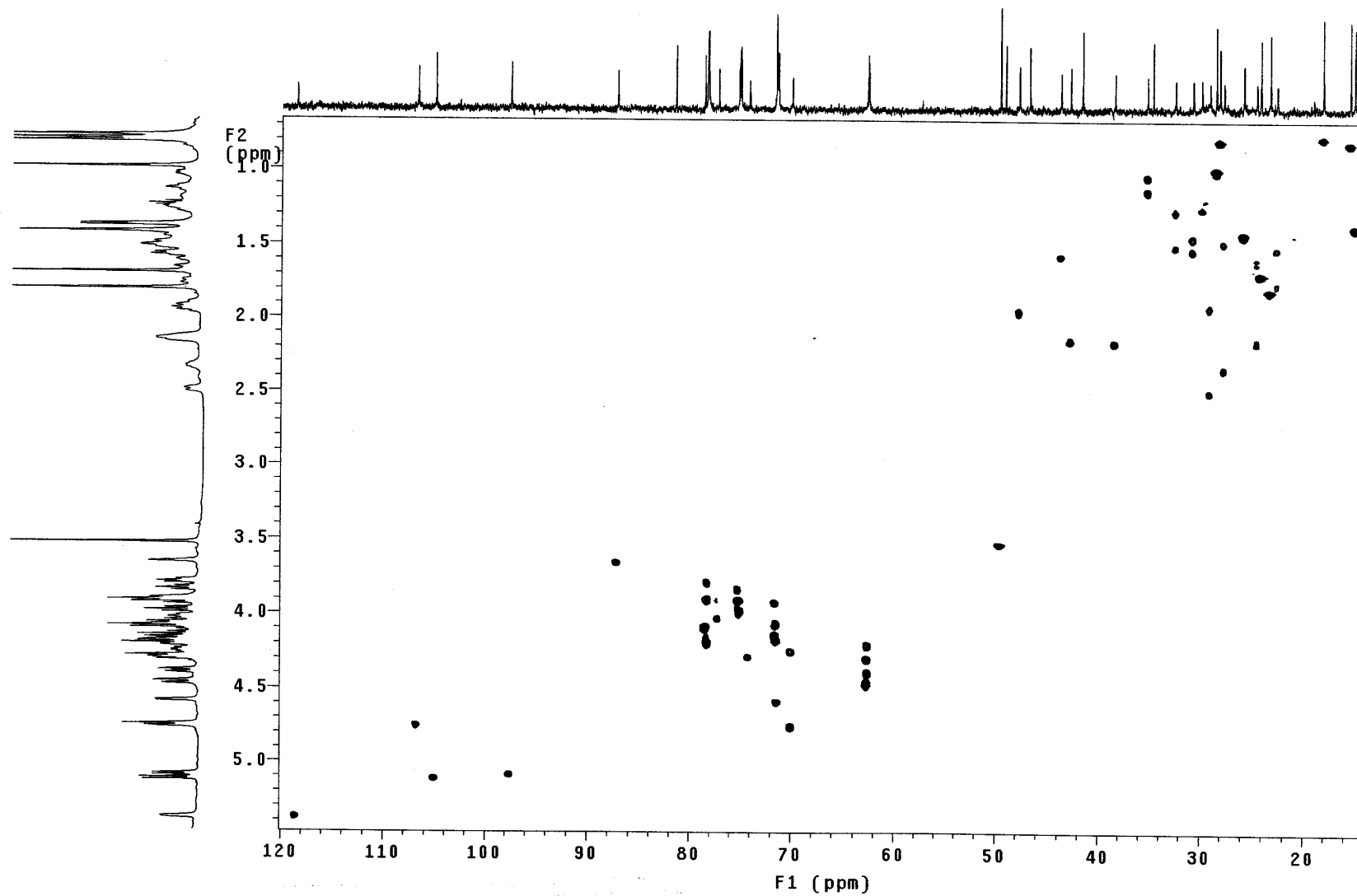
¹H NMR of Compound 5



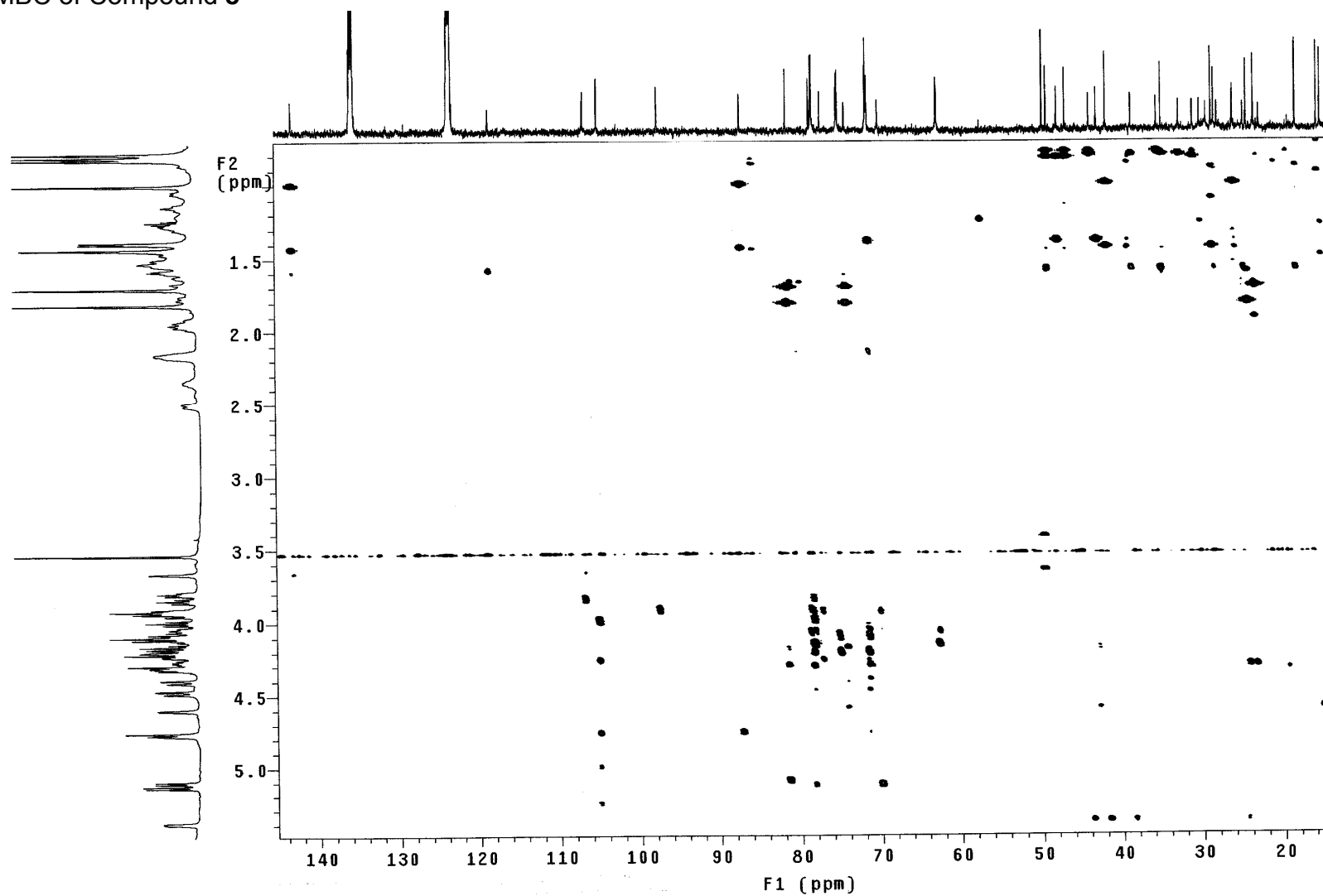
¹³C NMR of Compound 5



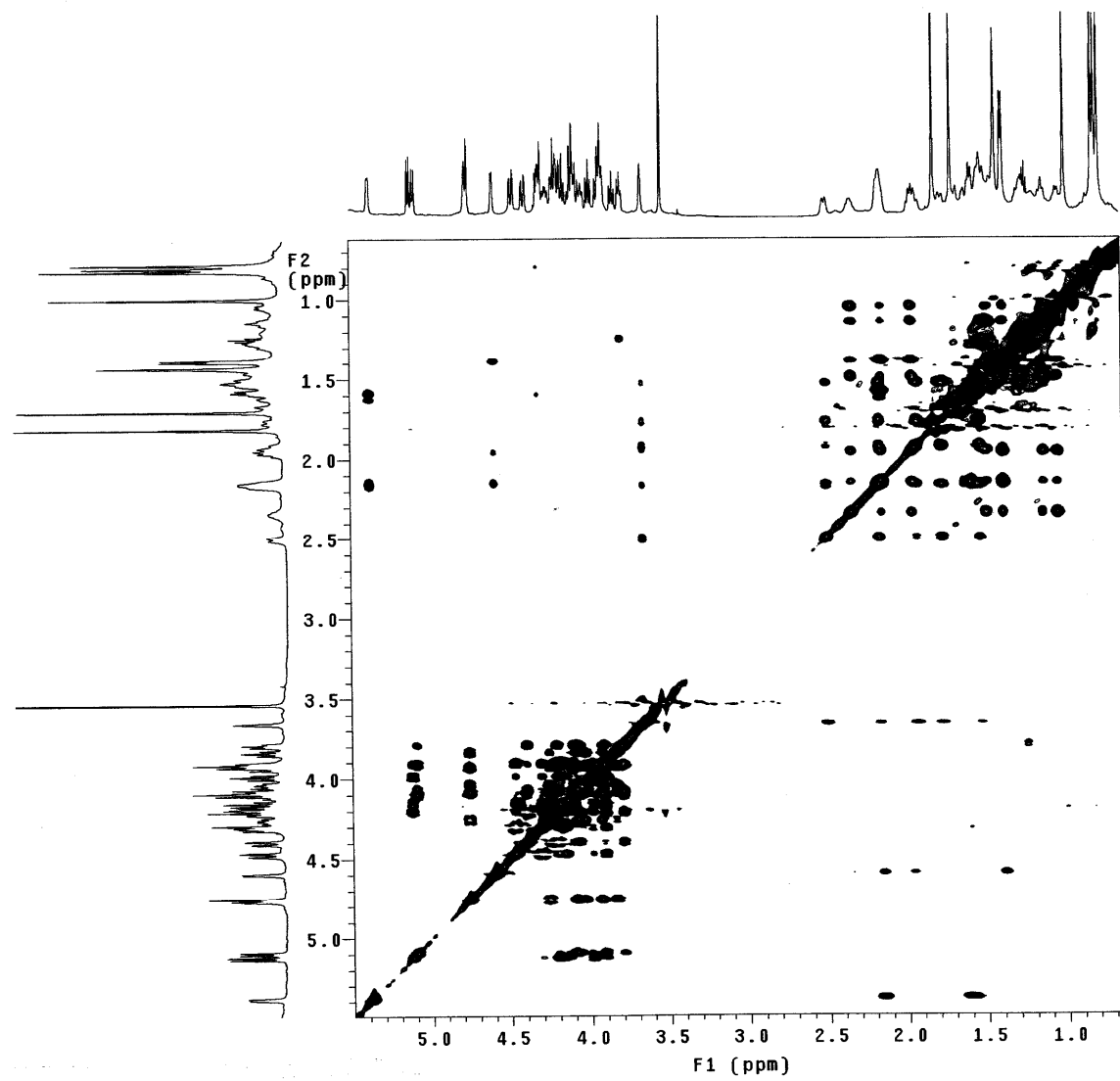
HSQC of Compound 5



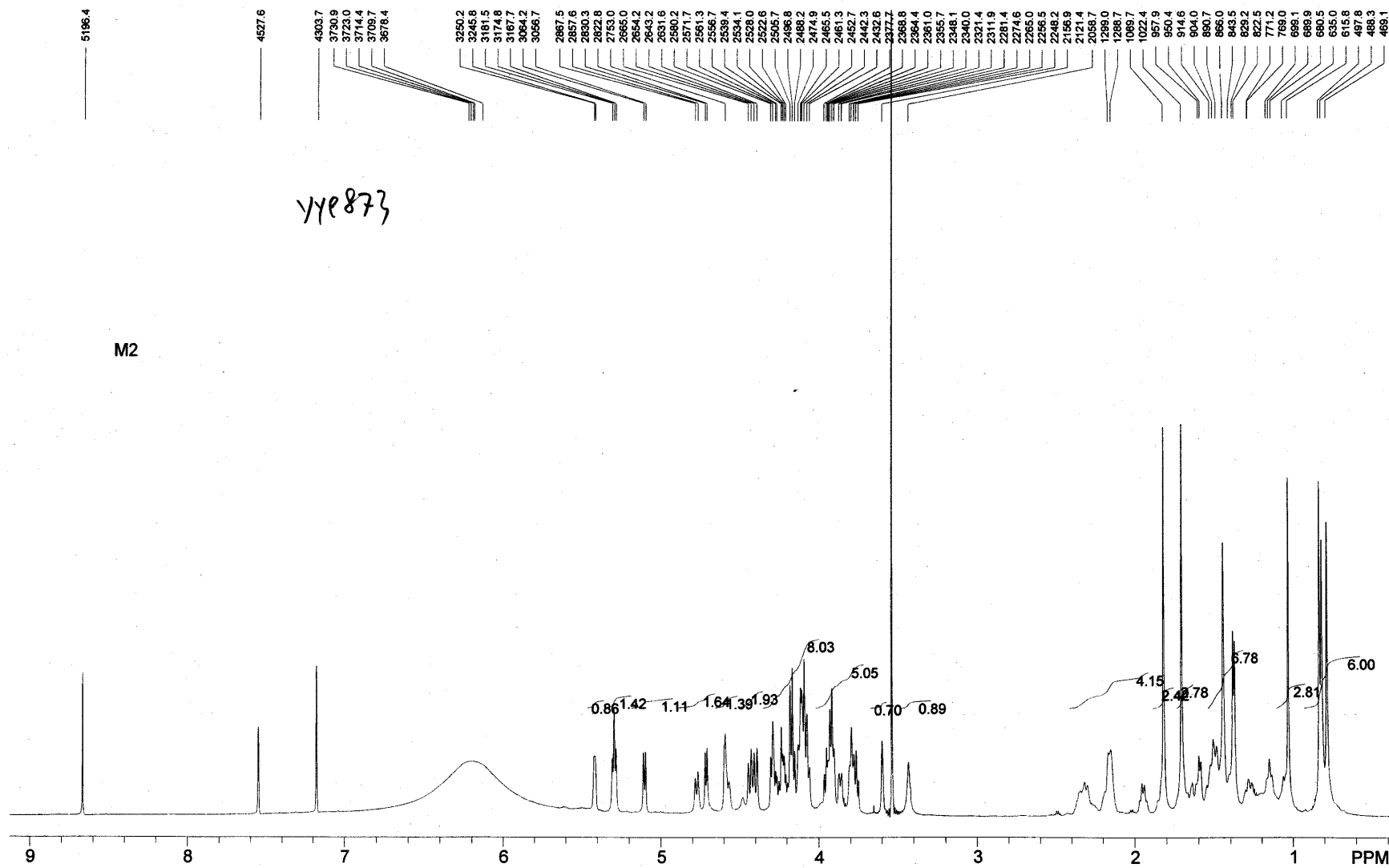
HMBC of Compound 5



TOCSY of Compound 5

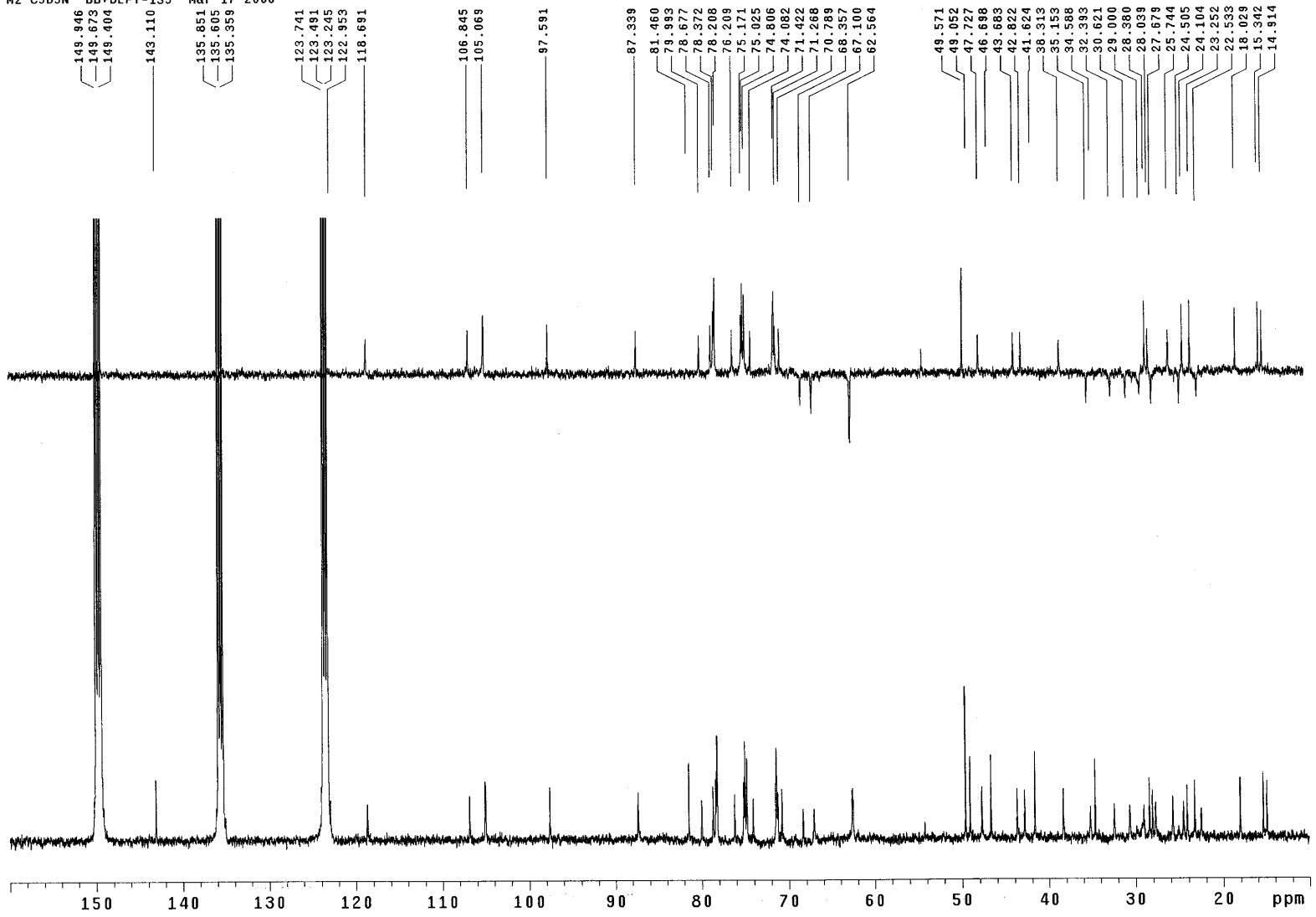


¹H NMR of compound 6

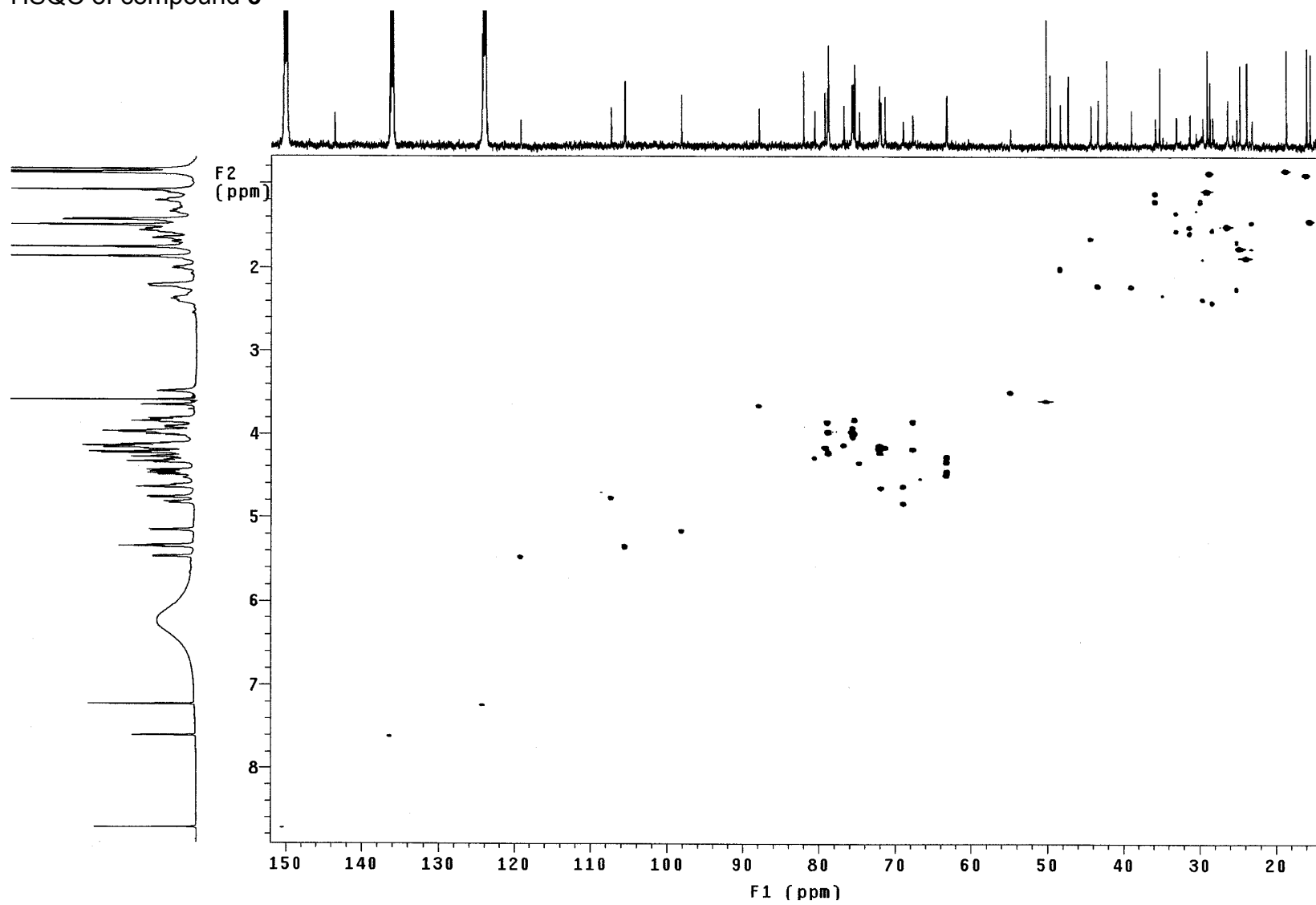


¹³C NMR of compound 6

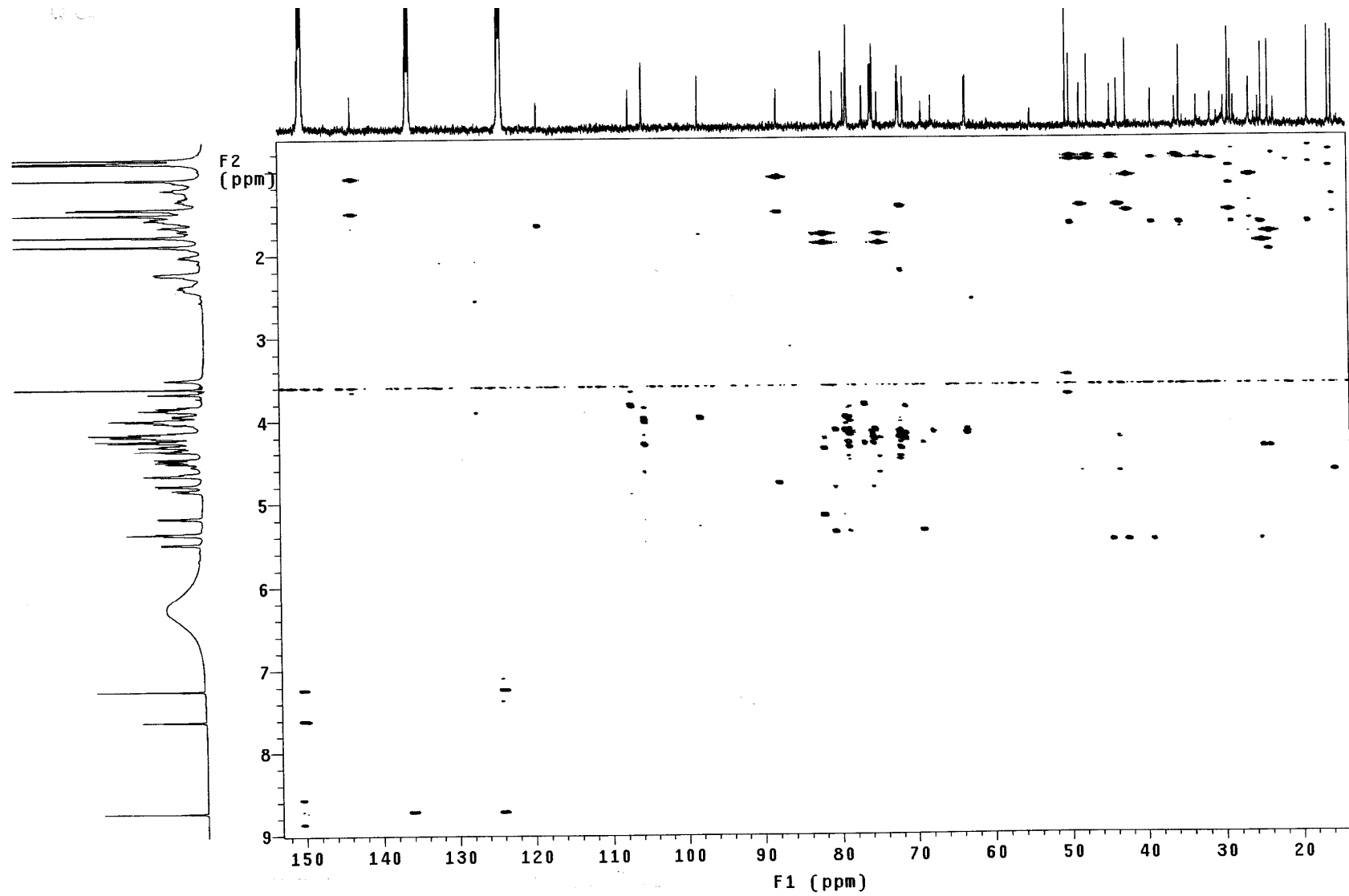
M2 C5D5N BB+DEPT-135 Mar 17 2006



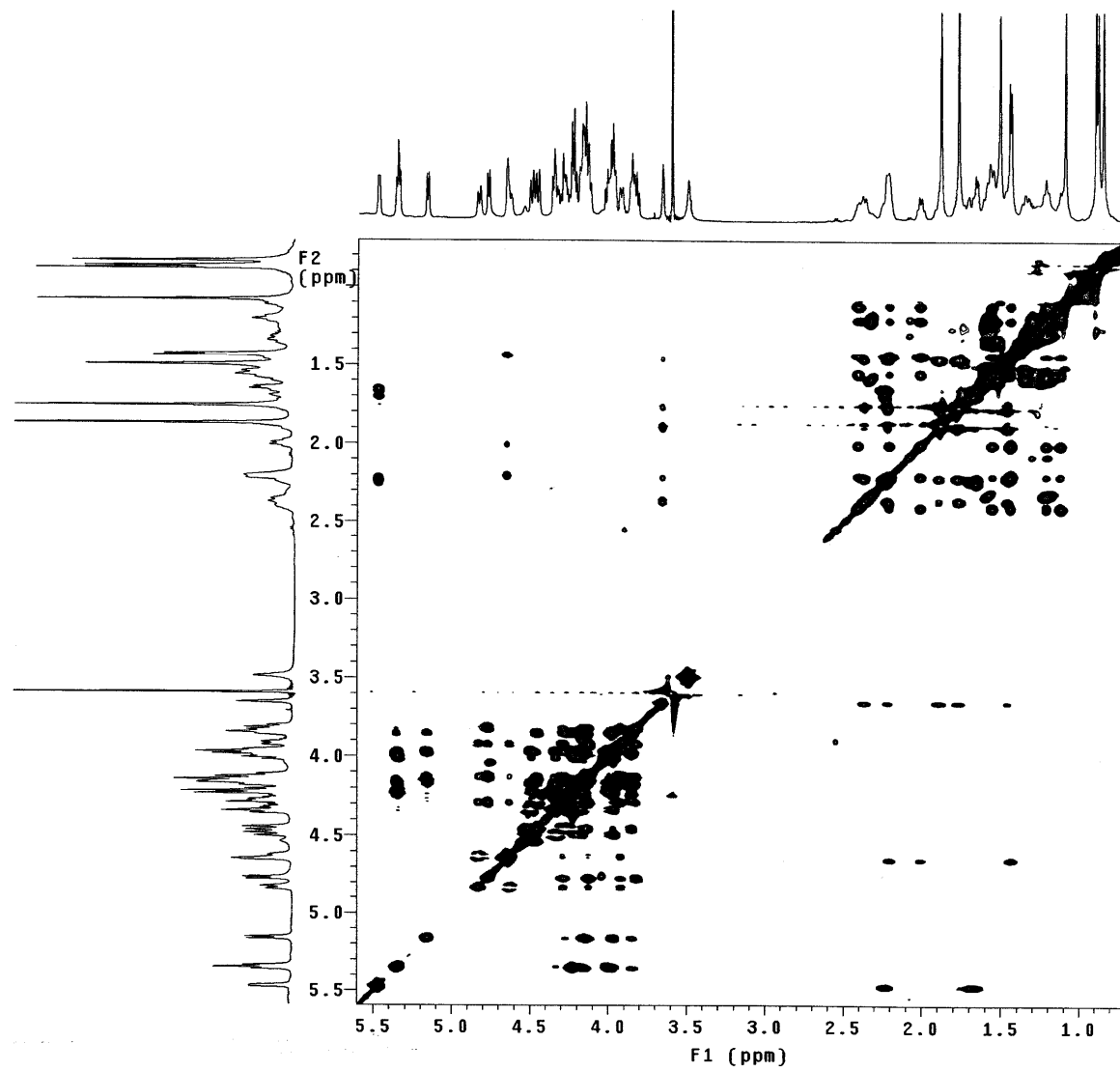
HSQC of compound 6



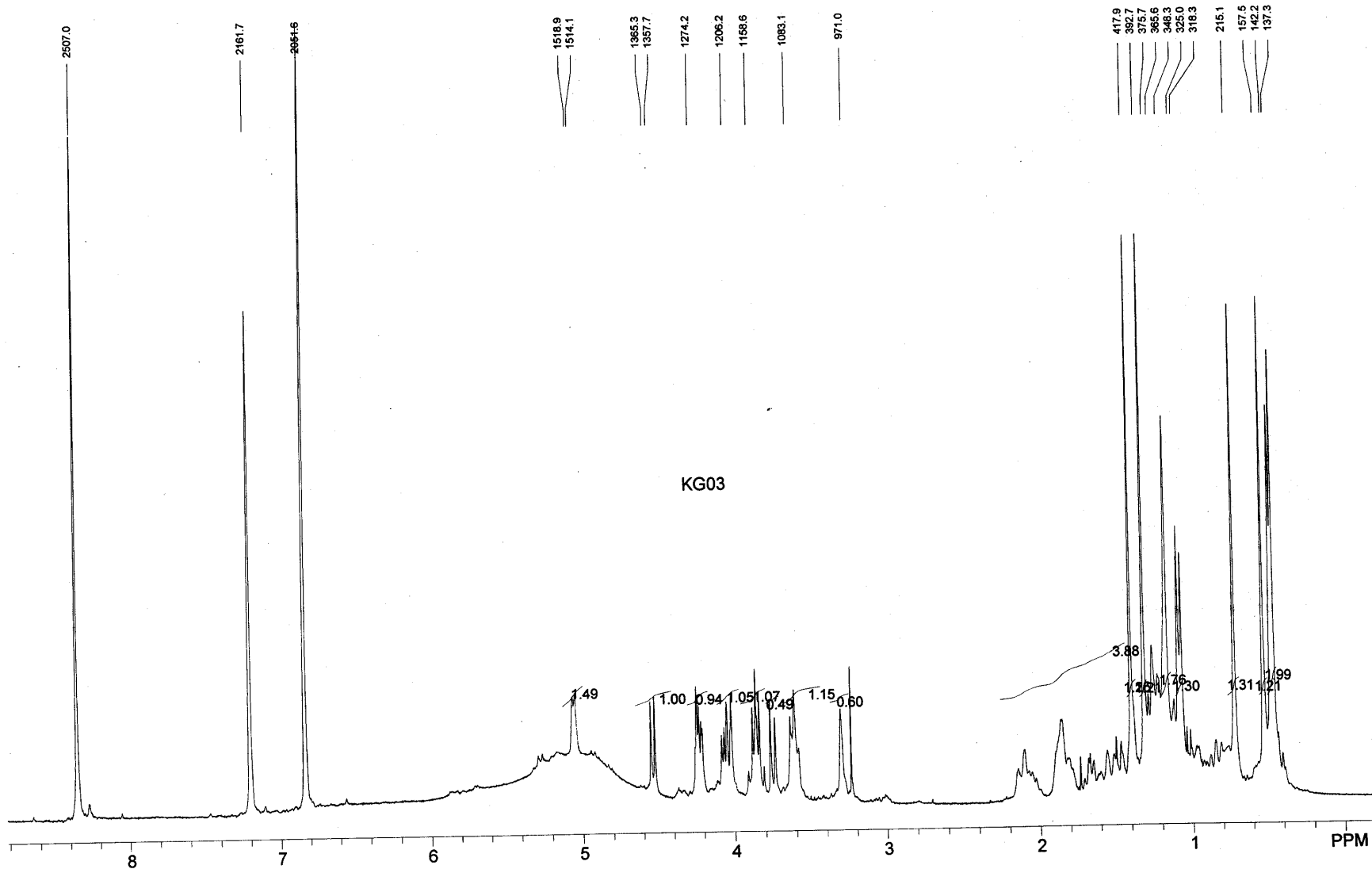
HMBC of compound 6



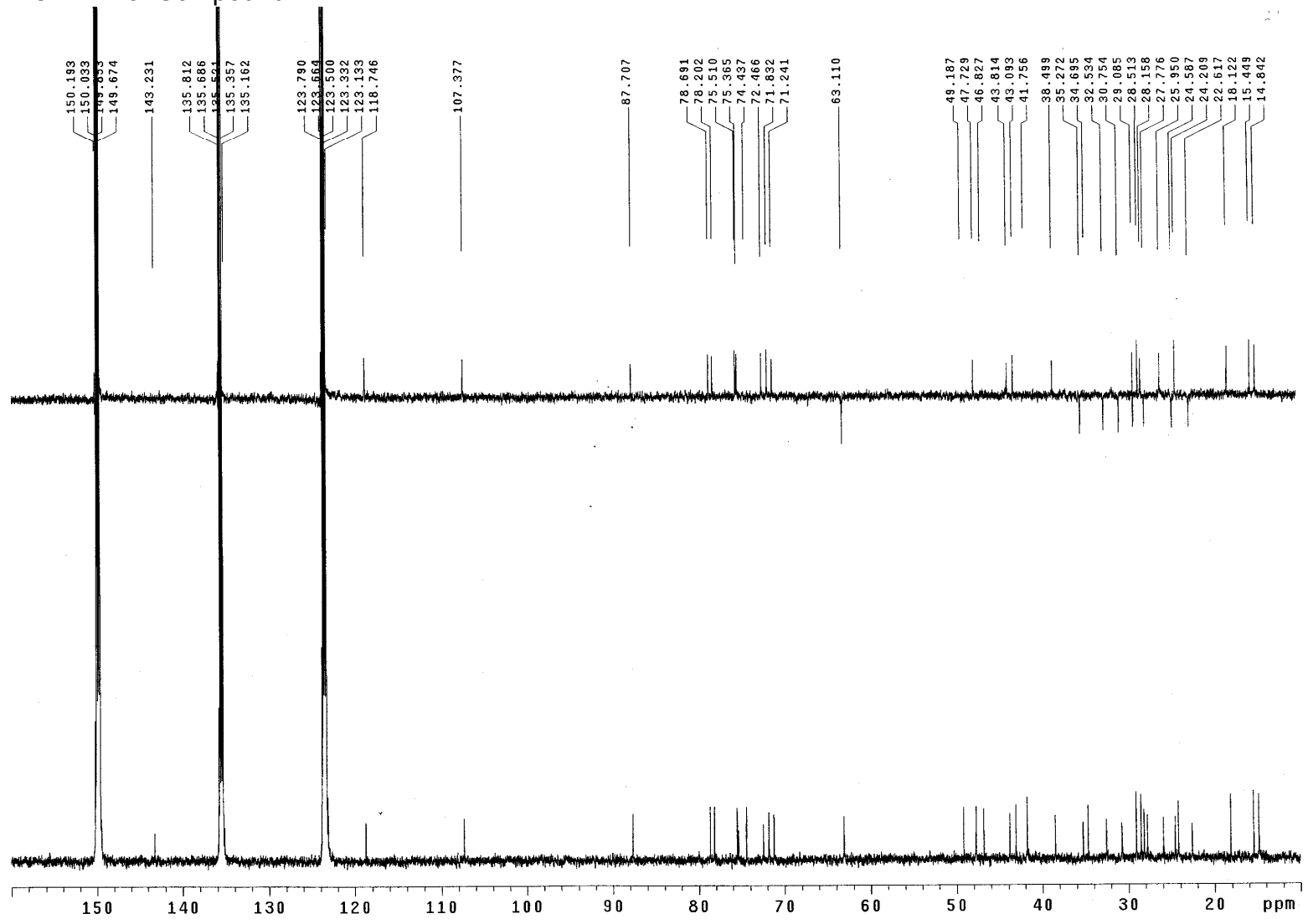
TOCSY of compound 6



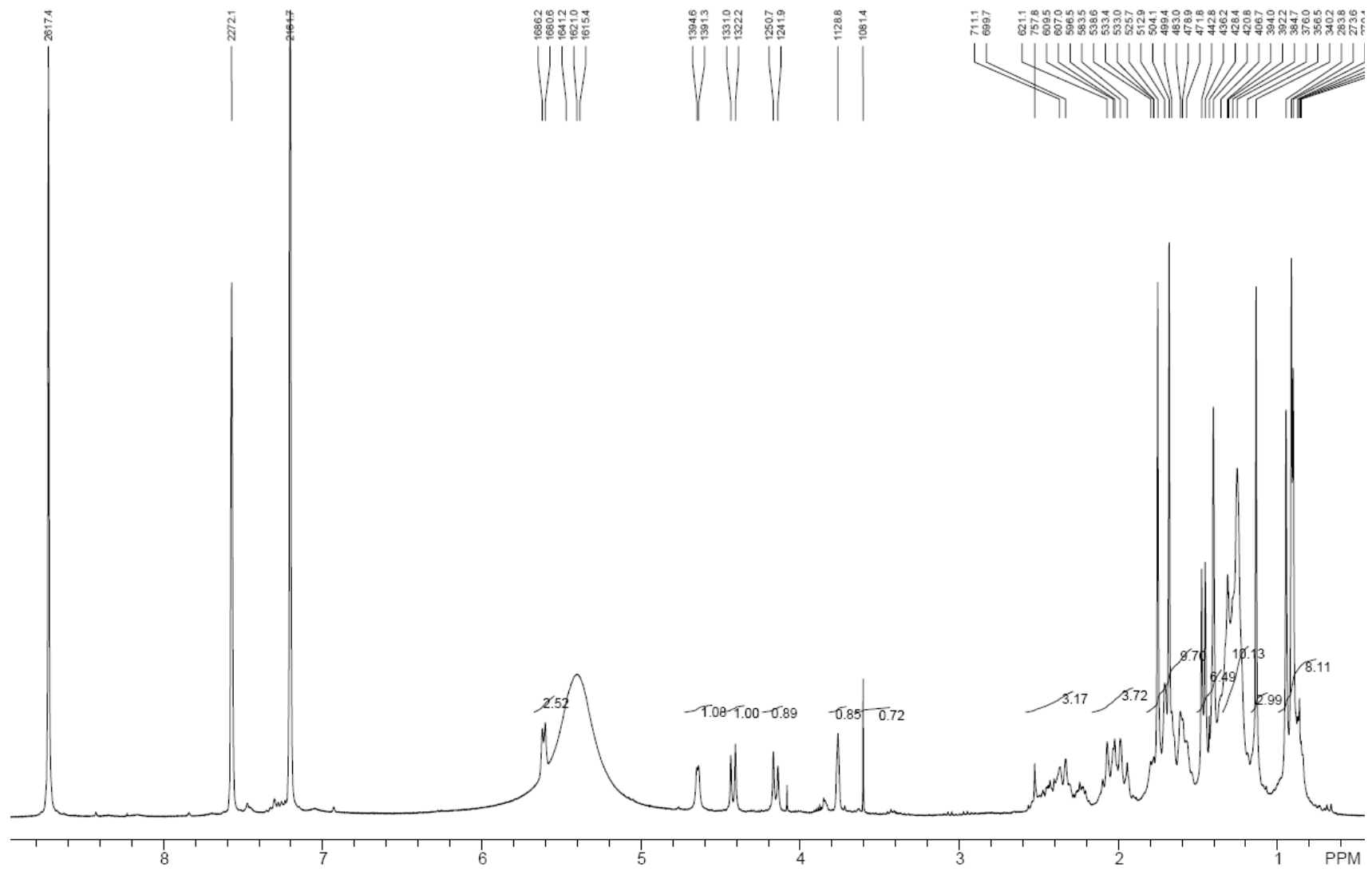
¹H NMR of Compound 7



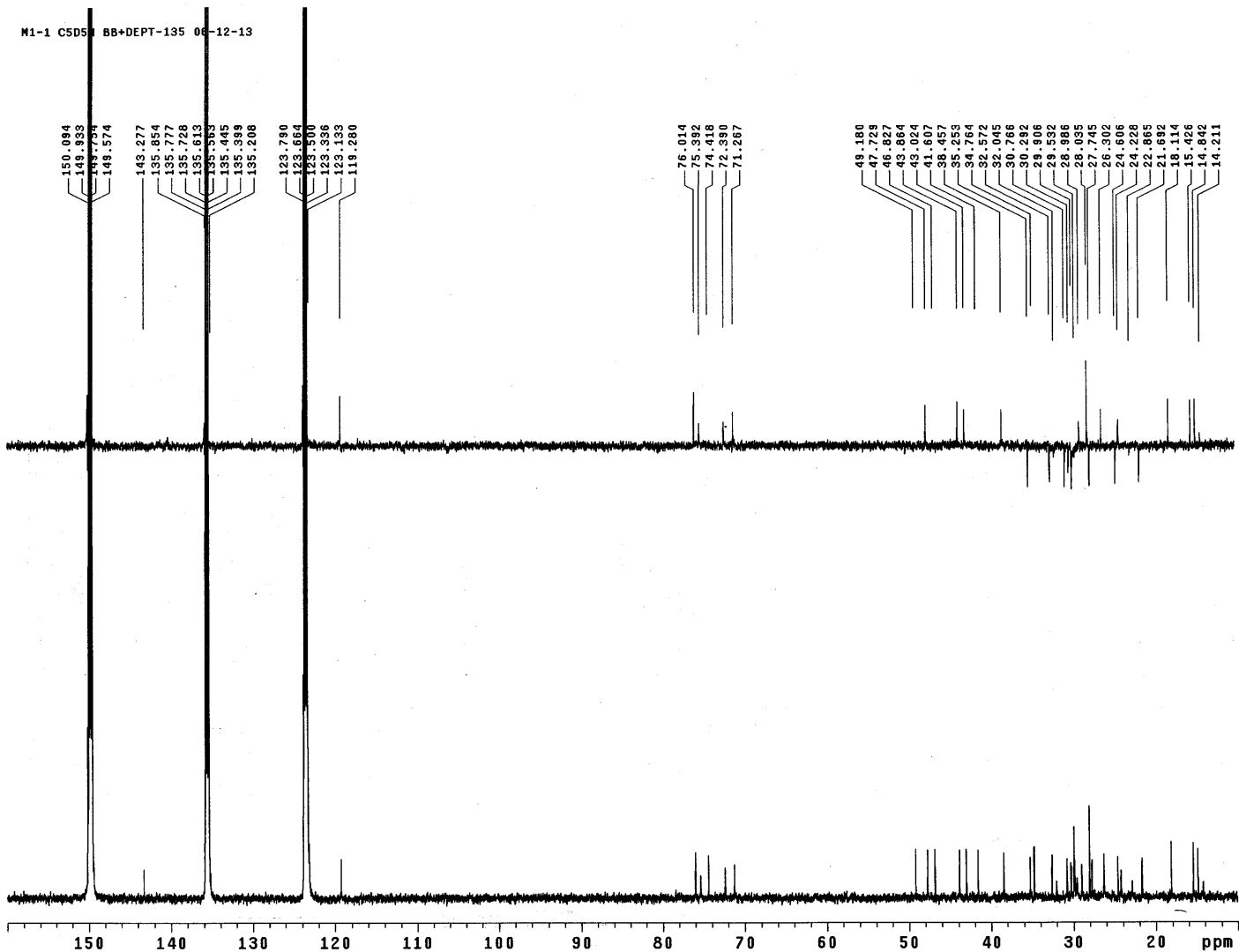
¹³C NMR of Compound 7



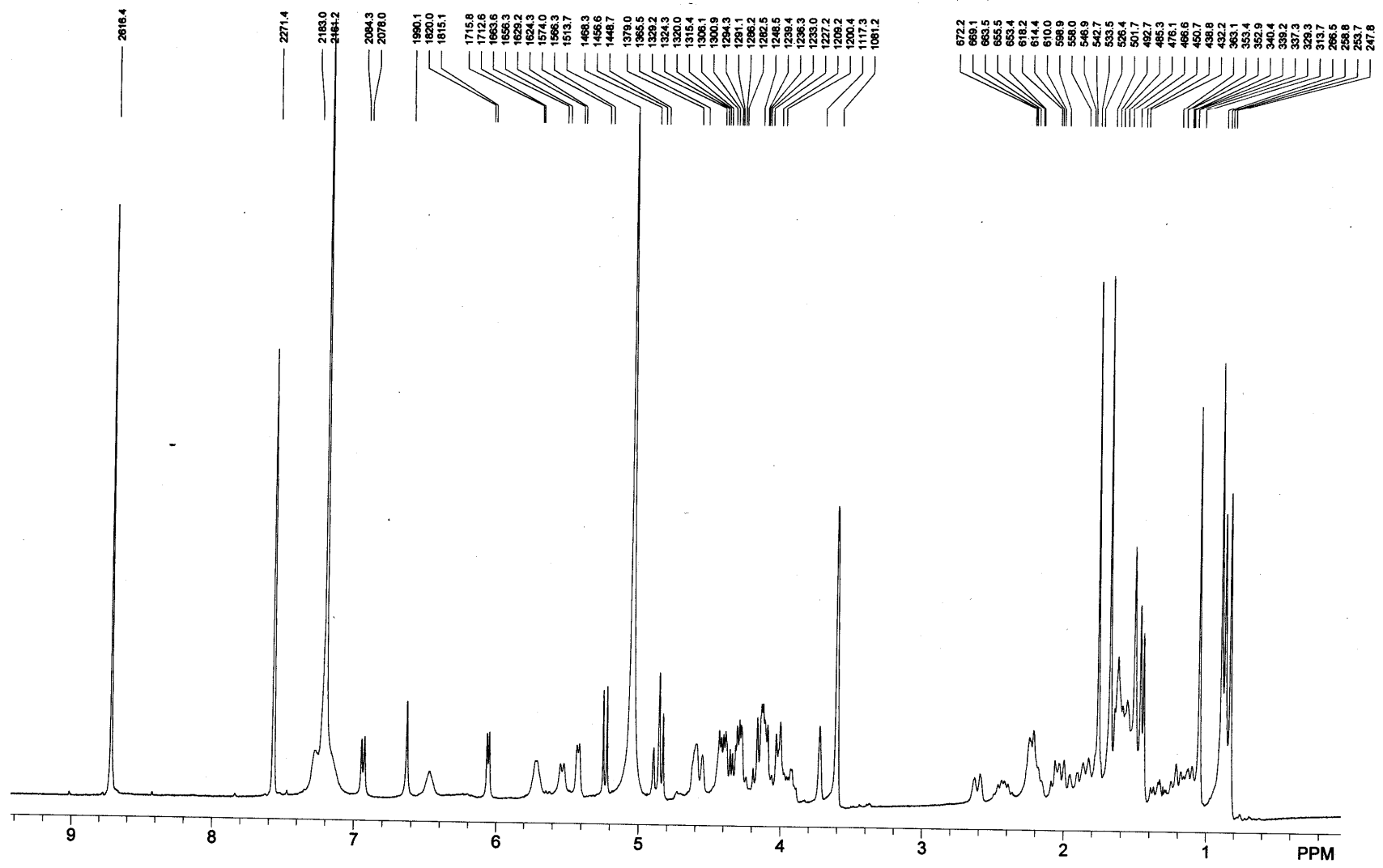
¹H NMR of Compound 8



¹³C NMR of Compound 8

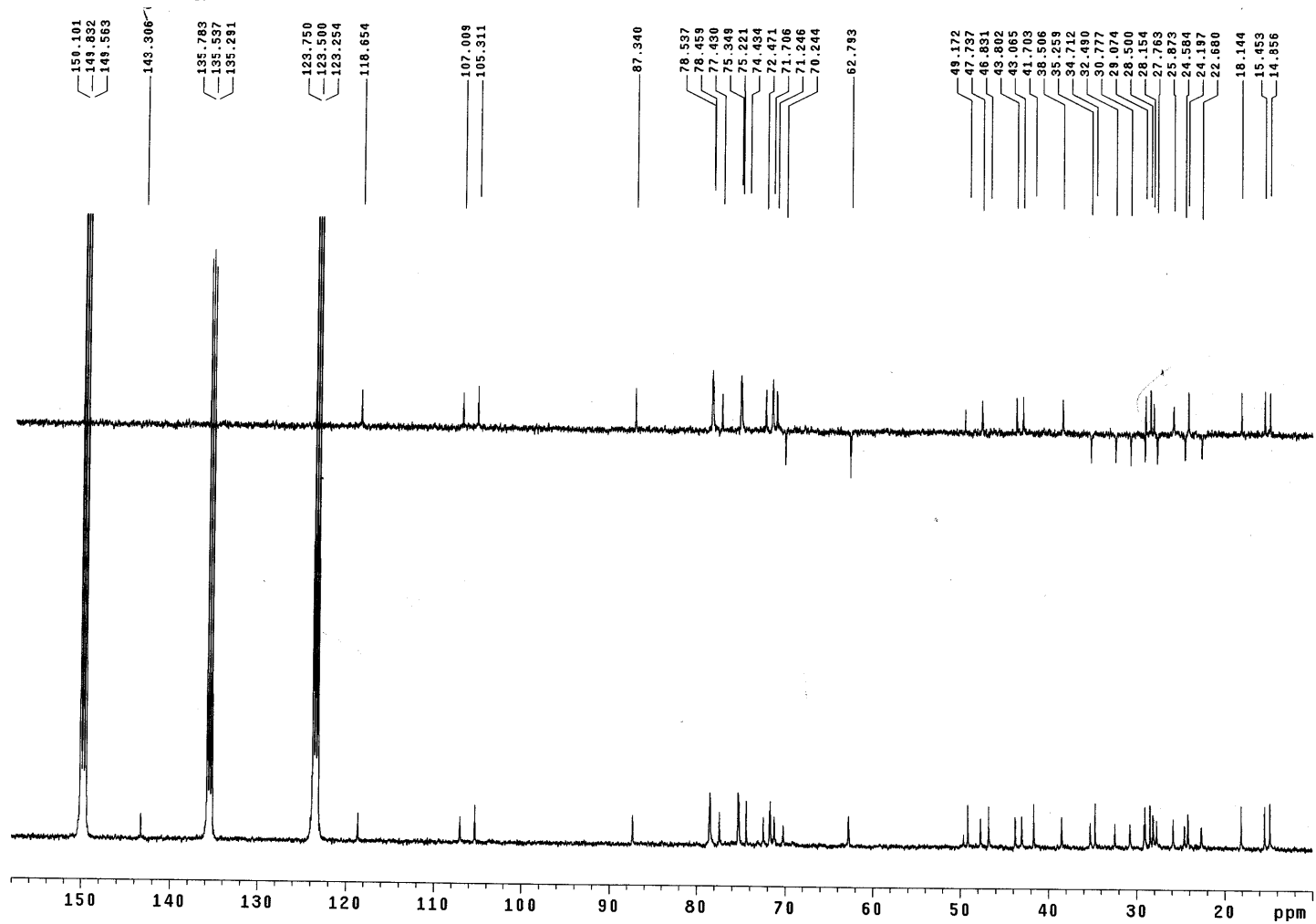


¹H NMR of Compound 9

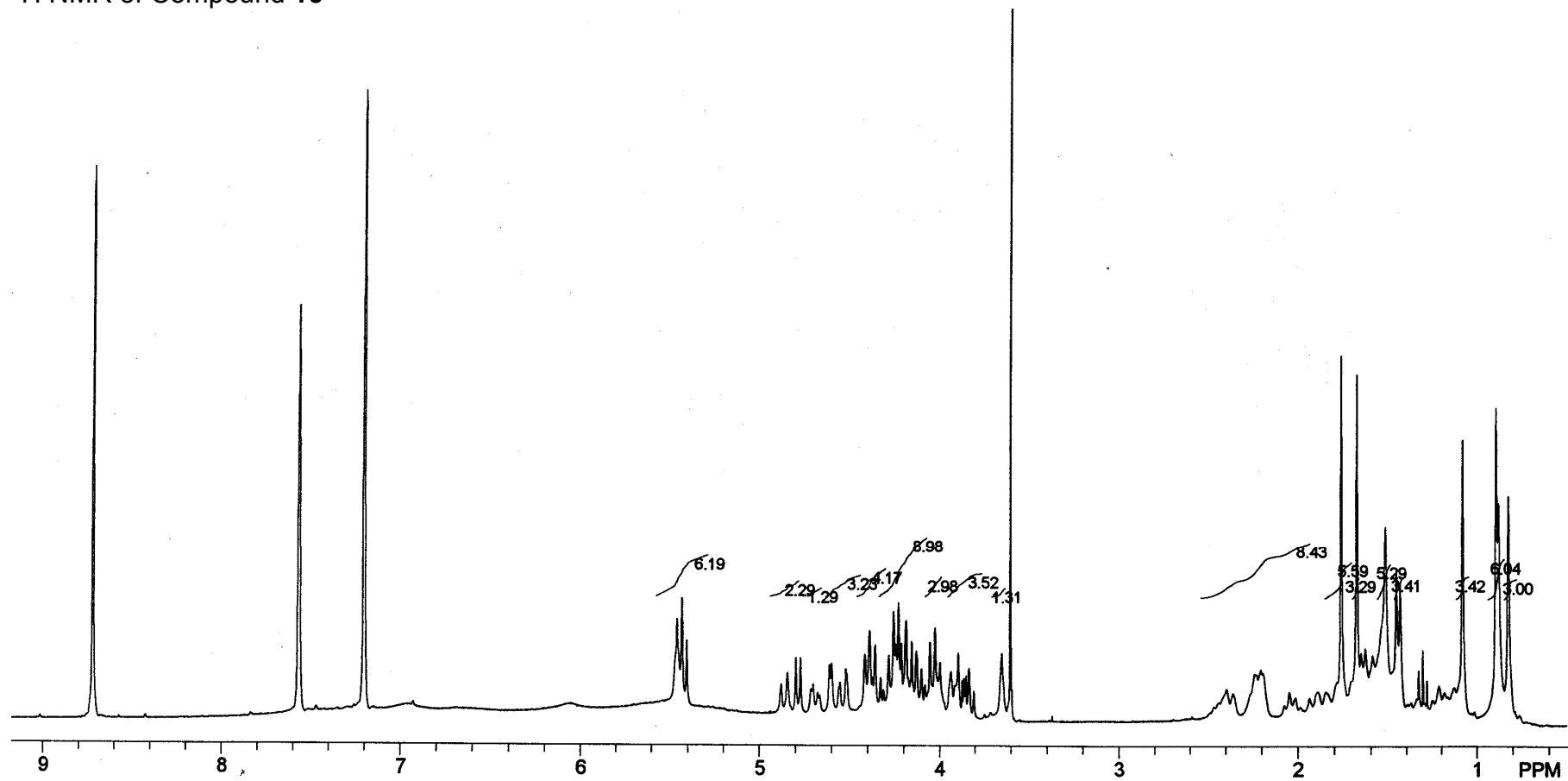


¹³C NMR of Compound 9

TB07 C505N BB+DEPT-135 05-4-19



¹H NMR of Compound 10



Positive ESIMS of Compound 10

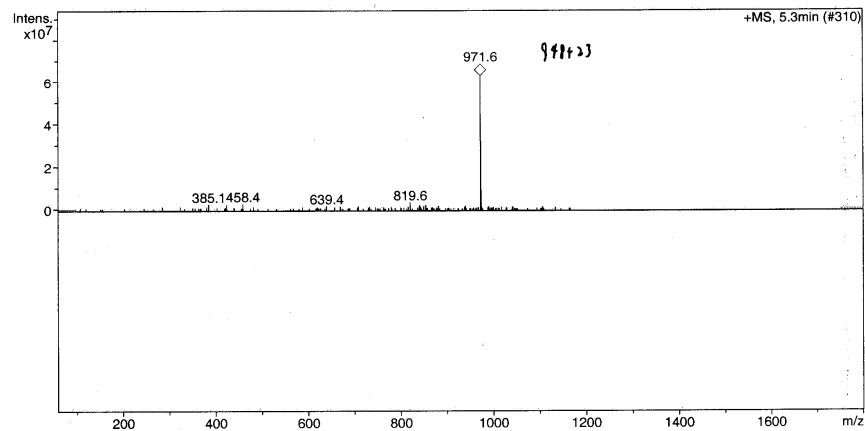
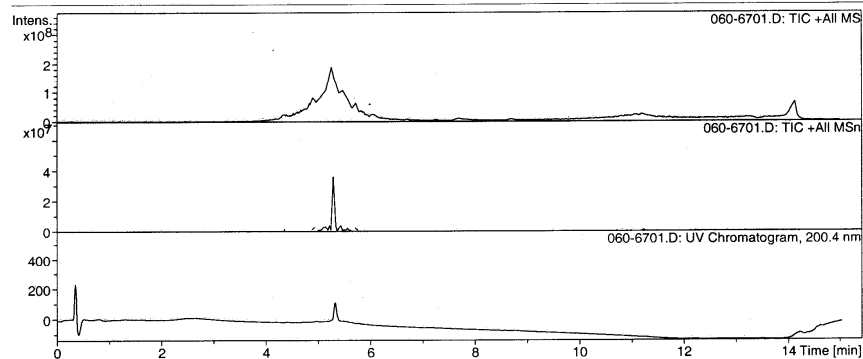
Display Report

Analysis Info

Analysis Name	060-6701.D	Acquisition Date	12/13/05 04:49:14
Method	Copy of SOPMSMSP.M	Operator	Administrator
Sample Name	yyc-KG102	Instrument	esquire3000plus_01005
Comment	□		

Acquisition Parameter

Ion Source Type	ESI	Ion Polarity	Positive	Alternating Ion Polarity	off
Mass Range Mode	Std/Normal	Scan Begin	100 m/z	Scan End	1750 m/z
Capillary Exit	160.0 Volt	Skim 1	40.0 Volt	Trap Drive	78.0
Accumulation Time	6410 μ s	Averages	3 Spectra	Auto MS/MS	on



Negative ESIMS of Compound 10

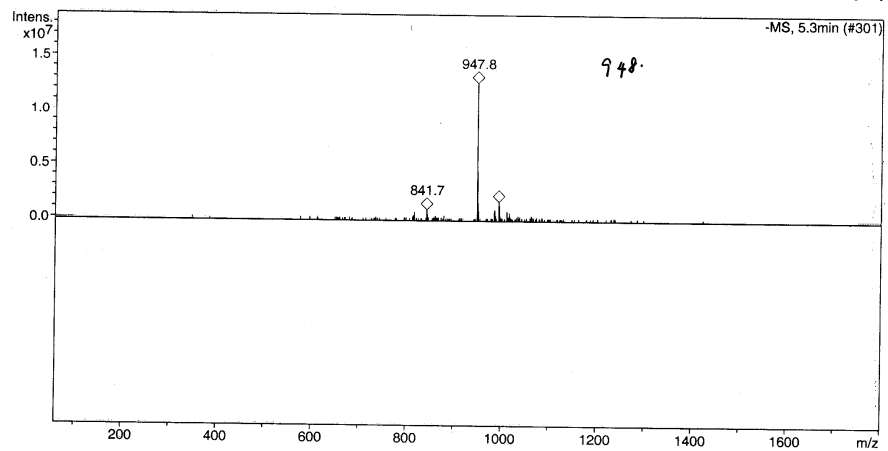
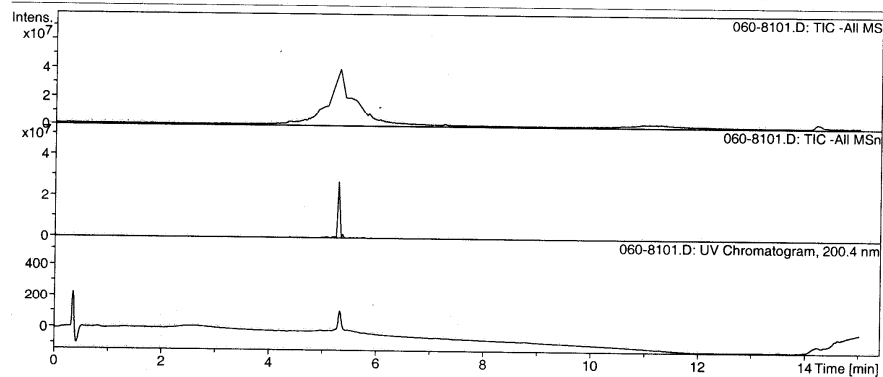
Display Report

Analysis Info

Analysis Name	060-8101.D	Acquisition Date	12/13/05 08:49:08
Method	Copy of SOPMSMS.N	Operator	Administrator
Sample Name	yyc-KG702	Instrument	esquire3000plus_01005
Comment	<input type="checkbox"/>		

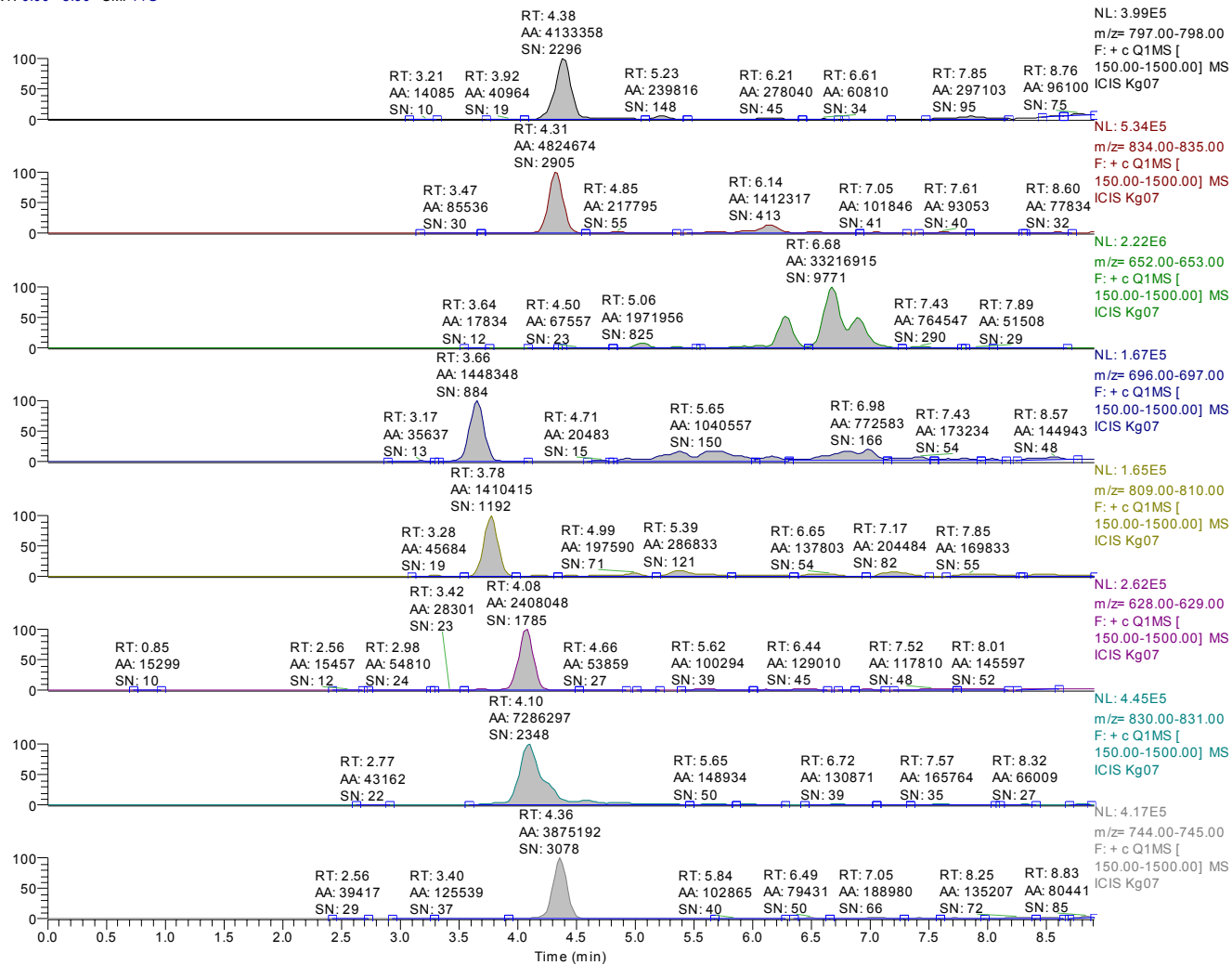
Acquisition Parameter

Ion Source Type	ESI	Ion Polarity	Negative	Alternating Ion Polarity	off
Mass Range Mode	Std/Normal	Scan Begin	100 m/z	Scan End	1750 m/z
Capillary Exit	-160.0 Volt	Skim 1	-40.0 Volt	Trap Drive	78.0
Accumulation Time	9429 μ s	Averages	3 Spectra	Auto MS/MS	on



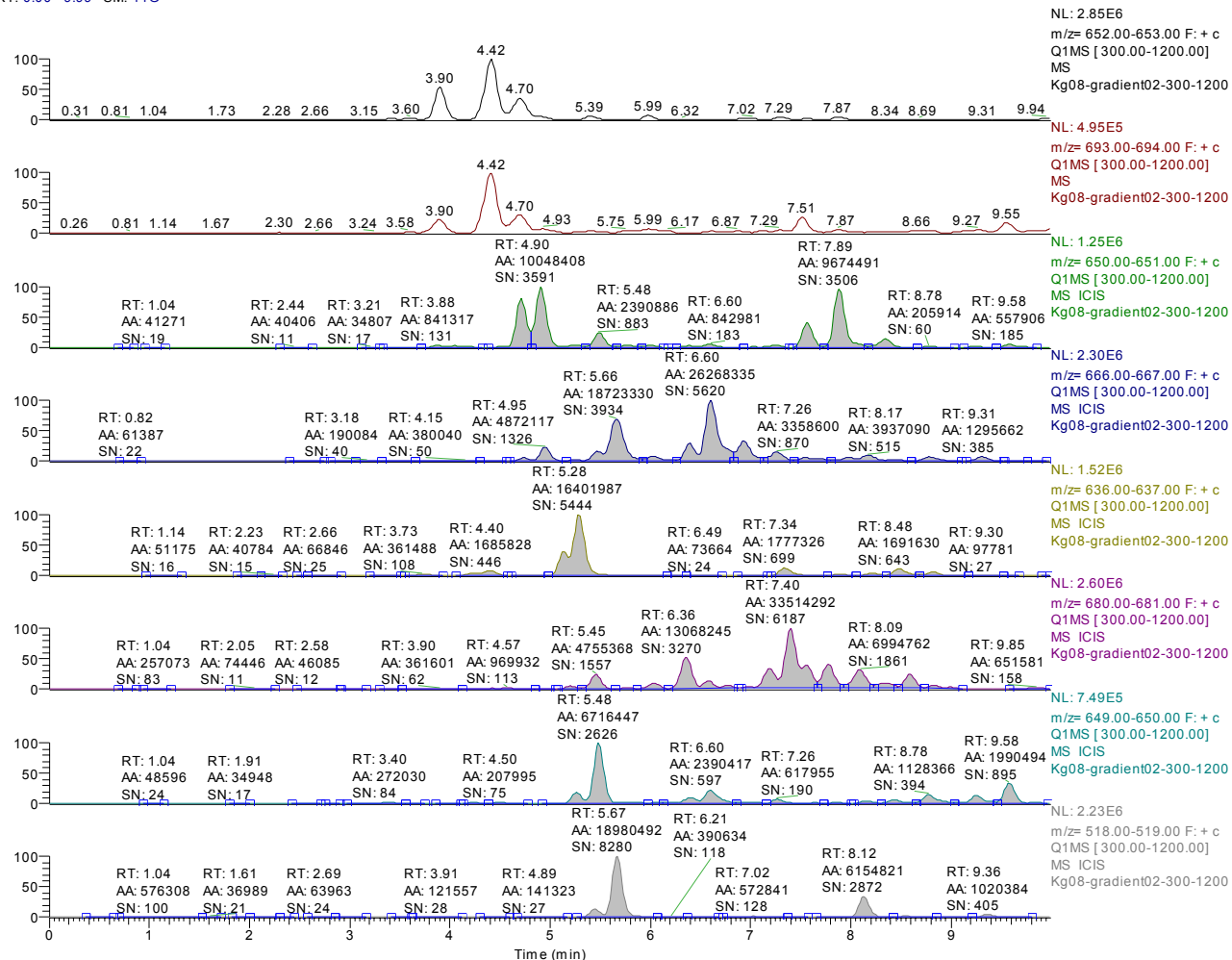
UPLC/ESIMS analysis of bitter melon extract (KG7)

RT: 0.00 - 8.90 SM: 11G



UPLC/ESIMS analysis of bitter melon extract (KG8)

RT: 0.00 - 9.99 SM: 11G



UPLC/ESIMS analysis of bitter melon extract (KG8, continued)

RT: 0.00 - 9.99 SM: 11G

